Received: 17 August 2022 | Revised: 22 August 2023 | Accepted: 5 October 2023

DOI: 10.1002/asmb.2829

RESEARCH ARTICLE

WILEY

# Examining the impact of critical attributes on hard drive failure times: Multi-state models for left-truncated and right-censored semi-competing risks data

**Jordan L. Oakley**[1] | **Matthew Forshaw**[2] | **Pete Philipson**[1] | **Kevin J. Wilson**[1]

[1]School of Mathematics, Statistics & Physics, Newcastle University, Newcastle upon Tyne, UK

[2]School of Computing, Newcastle University, Newcastle upon Tyne, UK

**Correspondence**
Jordan L. Oakley, School of Mathematics, Statistics & Physics, Newcastle University, Newcastle upon Tyne, UK.
Email: njo53@ncl.ac.uk

**Funding information**
Engineering and Physical Sciences Research Council

**Abstract**

The ability to predict failures in hard disk drives (HDDs) is a major objective of HDD manufacturers since avoiding unexpected failures may prevent data loss, improve service reliability, and reduce data center downtime. Most HDDs are equipped with a threshold-based monitoring system named self-monitoring, analysis and reporting technology (SMART). The system collects several performance metrics, called SMART attributes, and detects anomalies that may indicate incipient failures. SMART works as a nascent failure detection method and does not estimate the HDDs' remaining useful life. We define critical attributes and critical states for hard drives using SMART attributes and fit multi-state models to the resulting semi-competing risks data. The multi-state models provide a coherent and novel way to model the failure time of a hard drive and allow us to examine the impact of critical attributes on the failure time of a hard drive. We derive dynamic predictions of conditional survival probabilities, which are adaptive to the state of the drive. Using a dataset of HDDs equipped with SMART, we find that drives are more likely to fail after entering critical states. We evaluate the predictive accuracy of the proposed models with a case study of HDDs equipped with SMART, using the time-dependent area under the receiver operating characteristic curve (AUC) and the expected prediction error (PE). The results suggest that accounting for changes in the critical attributes improves the accuracy of dynamic predictions.

**KEYWORDS**

Critical states, hard disk drives, multi-state models, semi-competing risks, SMART

## 1 | INTRODUCTION

Manufacturers have an interest in the accurate assessment of product reliability. Consequently, there is a demand for models that can accommodate common failure patterns and methods to utilize the available data and properly account for uncertainty. Accurate models enable good decision-making in matters related to product life, including purchase

decisions, maintenance planning, and warranty prediction. To this end, products are being produced with modern technological developments, such as sensors or monitoring systems, that continuously record information about product health. Incorporating information collected by sensors has been shown to improve failure time predictions.[1]

A recent study based on data from Microsoft reports that 76%–95% of all failed components in data centers are hard drives.[2] Hard disk drives (HDDs) are the main reason behind server failures.[3] Consequently, research in hard drive failure prediction is critically important and has been extensively studied over the past decades. Predicting drive failures before they occur can inform us to take action in advance.

Most HDDs are equipped with a monitoring system named SMART (self-monitoring, analysis, and reporting technology). The primary function of SMART is to detect and report various indicators of drive reliability, with the intent of anticipating imminent hardware failures. At present, SMART is implemented inside most modern hard drives. However, as Murray et al.[4] and Lu et al.[5] reported, SMART alone does not lead to accurate predictions of failures. Moreover, in addition to whole-drive failures that make an entire drive unusable, modern drives can exhibit latent sector errors, reallocated sector counts, and many other read/write errors. The effect of such errors on the failure rates of hard drives is poorly understood.[6] Empirical observations show that the failure rates of hard drives increase after their first scan error.[7] First errors in reallocations and probational counts are also strongly correlated to higher failure probabilities.[7] Such errors weaken drives, but, to date, no paper has provided a measure of how much these errors weaken a drive. For example, how is the survival probability of a hard drive, over a forecast horizon of interest, impacted when a hard drive records a drive error, or multiple drive errors? We seek to provide answers to such questions.

Statistical and machine learning models have been proposed based on SMART attributes to improve failure prediction accuracy. Most papers approach hard drive failure prediction from a classification point of view, classifying drives as failed or not failed within a specific time horizon. Lu et al.[5] compare the prediction quality of machine learning models with different groups of SMART, performance and location features. The machine learning models classify hard drive failures 2–15 days in advance. Chhetri et al.[8] use machine learning methods and knowledge graphs to predict hard drive failures. Drives are classified one day in advance. Cahyadi and Forshaw[9] investigated the effect of class imbalance (for failed and healthy drives) in the Backblaze dataset,[10] and evaluated the effectiveness of three imbalance mitigation approaches, namely oversampling, severe undersampling and partial undersampling, to improve predictive accuracy of long short-term memory-based models. Cahyadi and Forshaw[9] used LSTM-based models to predict hard drive failures 10 days in advance. Botezatu et al.[11] used regularized greedy forest classifiers to predict hard drive failures 10–15 days in advance. Shen et al.[12] used part-voting random forests to predict hard drive failures. They compare part-voting random forests to classification trees and recurrent neural networks. The classifications are made one week in advance. Moreover, as mentioned by Lu et al.,[5] most papers classify hard drive failures using a prediction horizon of a few hours, days, or weeks. Spare parts planning, warranty planning, and maintenance planning can require predictions on a much longer time scale. It would be valuable to provide estimates, with uncertainty, of the survival probabilities and of the remaining useful life (RUL) distributions of drives.

Far fewer papers approach hard drive failure prediction from a probabilistic or RUL point of view, and these papers do not examine the impact of drive errors on hard drive failure times. Mittman et al.[13] proposed a hierarchical model to obtain the lifetime distributions of hard drives from different brands. Their approach borrows strength across brands with many observed failures to help make inferences for those brands with few failures. Their approach does not incorporate the attributes collected by SMART. Chaves et al.[14] obtained the RUL distribution estimates of HDDs using SMART attributes and a Bayesian Network. Lima et al.[15] presented a RUL estimation approach for hard drives using LSTM networks. Our goal is to propose a novel way to model the survival probabilities or failure times of hard drives, using data collected by SMART, and to concretely define the impact of drive errors on hard drive failure times.

As mentioned by Lu et al.,[5] SMART attributes do not always have strong predictive capabilities for hard drive failures over longer prediction horizons (i.e., predicting drive failure several weeks or months before the actual failure instead of a few hours or days in advance). This is primarily because the values of SMART attributes often do not change frequently enough during the period leading up to the failure, and the change is often noticeable only a few hours before the actual failure, especially in hard-to-predict cases. In this article, we define critical attributes and critical states for hard drives using SMART attributes. We utilize the probabilities of changes in critical attributes and the age of a hard drive to predict the probability of drive failure over time. We treat changes in critical attributes as drives entering critical states. Using the age of the drive and the state of the drive allows us to identify drives at risk of failure, even when the value of SMART attributes has been stationary for a long time. This article presents a general framework for modeling reliability field data collected from SMART for a population of hard drives, treating changes in critical attributes as drives entering critical (non-terminal) states. In this setting, the data collected by SMART can be considered semi-competing risks data.

Semi-competing risks refers to the setting where interest lies in the time-to-event for some terminal event, the observation of which may be subject to some non-terminal event(s).[16] In contrast to competing risks, where each of the outcomes under consideration is typically terminal, in the semi-competing risks setting, it is possible to observe multiple events in the same study unit, providing at least partial information on the joint distribution.[16,17] Toward the analysis of semi-competing risks data, the statistical literature has focused on three broad frameworks that seek to exploit the joint information on the times to the non-terminal and terminal events.[18] Those based on copulas;[16,19-21] those framed from the perspective of causal inference;[22,23] and, those based on the illness-death model.[17,24-28] In this article, we focus on the last of these approaches, for which the underpinning idea is that drives begin in some initial (healthy) state and may transition into the non-terminal (critical) state(s) and/or the terminal (failed) state. Analyses typically proceed through the development of models for transition-specific hazard functions, which dictate the rate at which units experience the respective events.

In the analysis of time-to-event outcomes, data are subject to left-truncation, or delayed entry, when units are enrolled into a study. In addition, units are subject to right-censoring. Left-truncation is common in large populations of units where units are required to be in a working state at an enrollment time in order to be included in a study. In this setting, sampling is biased since units are only included in the study if they are in a working state on entry. The analysis of left-truncated time-to-event data should apply statistical methods that account for this bias. Moreover, right-censoring is common in reliability studies when, due to advancements in technology, units are retired and replaced by newer technology, or because many units simply will not have failed at the end of the study. Not accounting for right-censoring will also produce biased estimates.

The contributions of this article are as follows. We define critical attributes and transient states, named critical states, for hard drives using data collected by SMART. We model the semi-competing risks data (entry to the critical state(s) and failure) using multi-state models. The proposed multi-state models provide a coherent and novel way to model the failure times of hard drives and allow us to statistically examine the impact of critical attributes on hard drive failure times. We illustrate how multi-state models can be used to obtain survival distributions and RUL distributions of hard drives using the age and state of a drive and compare our results to previous work by Mittman et al.[13] Using multi-state models we illustrate how to obtain dynamic predictions and show how survival probabilities are updated, using the age and state of a drive, as additional measurements of the age and critical attributes are recorded. Our motivating example concerns a dataset of hard drives, from data backup company Backblaze,[10] that is subject to left-truncation and right-censoring.

The structure of this article is as follows. In Section 2, we introduce the Backblaze hard drive dataset[10] used to motivate the multi-state models, through which we can examine the impact of critical attributes on hard drive failure times. In Section 3, we introduce the two-state model. We describe the data observed, derive the likelihood for hard drives subject to left-truncation and right-censoring, and propose the posterior predictive survival distribution for working drives, under the two-state model. In Section 4, we define critical attributes and critical states of hard drives. We propose the illness-death model, an extension of the two-state model, to describe the semi-competing risks data. We describe the data observed, derive the likelihood for hard drives subject to left-truncation and right-censoring, and propose the posterior predictive survival distributions for working drives, under the illness-death model. Furthermore, we introduce a four-state multi-state model, an extension of the illness-death model, referred to as the multi-state model. In Section 5, we introduce discrimination and calibration measures for model assessment for data subject to right-censoring. In Section 6, we model the failures ages of the Backblaze hard drives in the Bayesian framework using the two-state model, the illness-death model, and the multi-state model. We illustrate how multi-state models can be used to obtain posterior predictive survival probabilities and posterior predictive RUL distributions for hard drives using the age and state of a drive. We illustrate how posterior predictive survival distributions and posterior predictive RUL distributions can be used to define the impact of critical attributes on hard drive survival probabilities and failure times. In addition, we assess the performance of the two-state model, the illness-death model, and the multi-state model using discrimination and calibration measures through a simulation study. Section 7 concludes the paper with a discussion of our findings. Section A, in the supplementary material, provides supplementary tables and figures used in Section 6. Section B, in the supplementary material, provides alternative parameterizations of the Weibull distribution and introduces the generalized limited failure population (GLFP) model. In Section C, in the supplementary material, we describe the data observed, derive the likelihood for hard drives subject to left-truncation and right-censoring, and propose the posterior predictive survival distributions for working drives, under the multi-state model.

## 2 | MOTIVATING EXAMPLE: BACKBLAZE HARD DRIVE DATA

Backblaze is a company that offers cloud backup storage to protect against data loss. Since 2013, it has been collecting daily operational data, using SMART, on all of the hard drives operating at its facility. Every quarter Backblaze makes its hard drive data publicly available through its website.[10]

As of the first quarter of 2022, Backblaze was collecting and reporting data on 150 different drive models. Some drive models have been running since 2013 or before, while others were added at a later date. The number of drives and the number of failed drives vary by drive model; some models have no recorded failures.

Each day SMART takes a snapshot of each operational drive at Backblaze. This snapshot includes basic drive information, along with the SMART attributes reported by that drive. Consequently, for each drive, we have a time series for each recorded attribute. Each day, for each operational drive at Backblaze, SMART records: the date, the drive serial number, the drive-model, the capacity of the drive in bytes, an indicator denoting if the drive failed that day, and multiple SMART attributes.

Over time, the reporting technology is upgraded, and as a result, the number of recorded attributes changes over time. For example, between 2013 and 2014, SMART provided 80 columns of data per day, alongside basic drive information, for each hard drive. These columns correspond to the raw and normalized values of 40 different SMART attributes. From 2018 onwards, SMART provided 124 columns of data per day, alongside basic drive information, for each drive (corresponding to the raw and normalized values of 62 different SMART attributes).

The Backblaze hard drive failure ages are left-truncated and right-censored. When an observation is left-truncated, it would not have been observed if it had occurred prior to a particular time. Many Backblaze hard drives have a history prior to data collection, and hard drives that were in a failed state when data collection commenced are not included in the dataset. Hence, the ages of Backblaze hard drives at failure are left-truncated. In addition, it is rare that all drives in a study are observed until failure. If a drive has not failed when the study ends, it is considered right-censored. Right-censoring puts a lower bound on the failure age. Left-truncation and right-censoring must both be incorporated to avoid biased estimates.

In this article, we extend the methods proposed by Mittman et al.[13] to incorporate the attributes collected by SMART. We compare our results to the results presented in Mittman et al.,[13] sec. 4.2. More specifically, to illustrate the multi-state models proposed in this article, we present an analysis of drive model 14. Drive-model 14 was a hard drive used by Backblaze up to (and including) the last quarter of 2015. Between 2013 and 2016, Backblaze deployed 4707 model 14 drives.

## 3 | TWO-STATE MODEL

A standard survival or reliability analysis can be thought of as a two-state model, where drives start in the healthy state (state 0) and eventually transition to the failed state (state 1). Let $T$ denote the failure age. We assume a two-state model for each individual drive of the form shown in Figure 1. The two-state model is characterized by the transition hazard

$$\lambda(t|\boldsymbol{\theta}) = \lim_{\Delta \to 0} \frac{\Pr(T \in [t, t+\Delta) | T \geq t, \boldsymbol{\theta})}{\Delta}, \text{ for } t > 0, \tag{1}$$

where $\lambda$ is the hazard rate (transition intensity) of the $0 \to 1$ transition, $\boldsymbol{\theta}$ is a vector of model parameters associated with $\lambda$, and states 0 and 1 are healthy and failed states, respectively.

### 3.1 | Observed data under the two-state model

Let $T_i$ denote the true failure age for drive $i$ and let $L_i$ and $C_i > L_i$ denote the left-truncation age (the age of the drive at study entry) and right-censoring age for drive $i$, respectively, which we assume are independent of $T_i$. Moreover, let

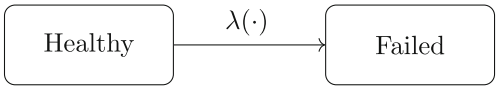


**FIGURE 1** A two-state model.

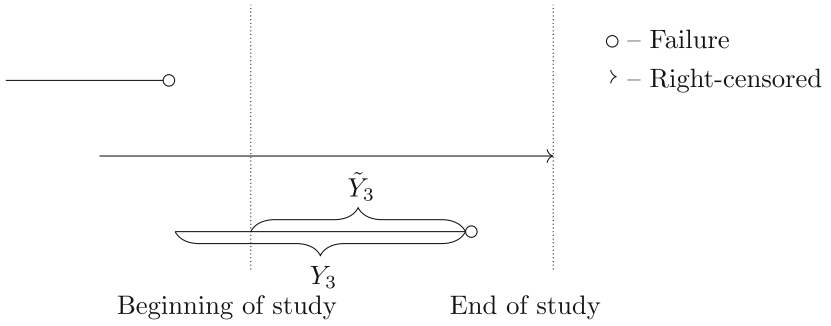


**FIGURE 2** Two possible life histories under the two-state model and an example drive not included in the dataset.

$Y_i = \min(T_i, C_i)$ denote the observed failure age for drive $i$, with failure indicator $\delta_i = I\{T_i \leq C_i\}$, where $I(\cdot)$ is an indicator function, which is equal to 1 if $T_i \leq C_i$ and 0 otherwise. The Backblaze hard drives are left-truncated and satisfy the recruitment criterion $L_i < Y_i$. That is, hard drives that failed before the study commenced are not included in the dataset. The observed data for the $i$th drive is $\mathcal{D}_i = \{l_i, y_i, \delta_i\}$. In words, for drive $i$, we observe the age at study entry, $l_i$; an indicator function, $\delta_i$, which is equal to 1 if drive $i$ failed and is equal to 0 if drive $i$ is right-censored (has not failed); and the observed failure age, $y_i$. If drive $i$ failed, we observe the true failure age, and if drive $i$ is right-censored, we observe the right-censoring age (a lower bound on the true failure age).

Figure 2 provides a schematic representation of two possible life histories observed under the two-state model with left-truncation and right-censoring, and a description of a drive that is not included in the dataset since it did not satisfy the recruitment criterion, $L_i < Y_i$. We illustrate the difference between the failure age and the failure time using scenario 3 in Figure 2. The failure age of drive 3 is denoted $Y_3$ and the failure time is denoted $\tilde{Y}_3$. Drive 1 failed prior to the start of the study and was not included in the dataset. Drive 2 is right-censored at the end of the study. Drive 3 failed prior to the end of the study.

## 3.2 | Likelihood under the two-state model

The observed data take the form $\mathcal{D}_n = \{l_i, y_i, \delta_i; i = 1, \ldots, n\}$. Assuming the ages of the drives are independent, the censoring process is non-informative about $T$,[29] and that we do not have any knowledge about the truncation distribution,[29] the likelihood for the data, $\mathcal{D}_n$, can be written as follows:

$$L(\boldsymbol{\theta}; \mathcal{D}_n) = \prod_{i=1}^{n} \frac{S(y_i|\boldsymbol{\theta})\lambda^{\delta_i}(y_i|\boldsymbol{\theta})}{S(l_i|\boldsymbol{\theta})}, \tag{2}$$

as provided by Mittman et al.,[13] where $S(y_i|\boldsymbol{\theta}) = \exp\left(-\int_0^{y_i} \lambda(u|\boldsymbol{\theta})du\right)$ is the probability that drive $i$ does not transition from $0 \rightarrow 1$ by age $y_i$.

## 3.3 | Posterior predictive survival distribution under the two-state model

Under the two-state model, the posterior predictive survival distribution is given by

$$\Pr(T \geq \gamma + s|T > \gamma, \mathcal{D}_n) = \int \Pr(T \geq \gamma + s|T > \gamma, \boldsymbol{\theta}) p(\boldsymbol{\theta}|\mathcal{D}_n) d\boldsymbol{\theta}, \tag{3}$$

where

$$\Pr(T \geq \gamma + s|T > \gamma, \boldsymbol{\theta}) = \frac{S(\gamma + s|\boldsymbol{\theta})}{S(\gamma|\boldsymbol{\theta})}, \tag{4}$$

and

$$p(\theta|\mathcal{D}_n) \tag{5}$$

is the posterior distribution of the two-state model parameters given the observed data, $\mathcal{D}_n$.

## 4 | MULTISTATE MODELS

In this section, we define critical attributes and critical states for hard drives using data collected by SMART. We propose the illness-death model, an extension of the two-state model, to describe the semi-competing risks data. We describe the data observed, derive the likelihood for hard drives subject to left-truncation and right-censoring, and propose the posterior predictive survival distributions for working drives, under the illness-death model. Furthermore, we introduce a four-state multistate model, an extension of the illness-death model, referred to as the multi-state model.

### 4.1 | Attribute selection

Backblaze uses five SMART attributes as a means of helping determine if a drive is going to fail.[30,31] Namely, SMART 5, the reallocated sectors count; SMART 187, the reported uncorrectable errors; SMART 188, command timeout; SMART 197, the current pending sector count; and SMART 198, the uncorrectable sector count. When the raw value for at least one of these five attributes is greater than zero, Backblaze has a reason to investigate.[30,31]

Rincón et al.[30] investigated three different machine learning models using Backblaze data. They performed a statistical analysis to reduce the number of SMART attributes to consider and to eliminate irrelevant variables (variables without any relationship to drive failure). Their trend test identified six attributes to be used in the machine learning models. Namely, SMART 196, the reallocation event count, and the five attributes used by Backblaze.

Ma et al.[6] designed RAIDSHIELD, consisting of PLATE and ARMOR. PLATE monitors individual drive health by tracking the number of reallocated sector counts (SMART 5) and proactively detecting unstable drives. ARMOR utilizes joint failure probabilities to quantify and predict how likely a RAID group (multiple hard drives grouped together to decrease the risk of data loss) is to face multiple simultaneous drive failures. The joint failure probabilities depend on the number of reallocated sector counts (SMART 5). Their results show that the accumulation of reallocated sectors is correlated with a higher probability of failure.

Following from Ma et al.,[6] Rincón et al.,[30] and Backblaze[31] we consider SMART attributes 5, 187, 188, 197, and 198. From herein these SMART attributes are referred to as critical attributes. We note that SMART 196 is missing for all hard drives in our dataset.

### 4.2 | Model for critical attributes

A parametric model for each critical attribute process is needed for the purpose of prediction. Figure 3 (left) depicts the longitudinal profile of the reallocated sector count (SMART 5) for five example hard drives. Figure 3 (right) depicts the longitudinal profile of the reported uncorrectable errors (SMART 187) for five example hard drives. From Figure 3, we can see that there is no clear trend in the reallocated sector count over time, nor in the reported uncorrectable errors over time (other than both being non-decreasing).

Table 1 provides summary statistics for the five critical attributes for model 14 hard drives. More specifically, Table 1 provides, for each critical attribute, quantiles of the time between jumps (nonzero increases), in hours (for hard drives with at least two nonzero values); quantiles of the size of the first nonzero jump (for hard drives with at least one nonzero value); and quantiles of the number of nonzero jumps (for hard drives with at least one nonzero value). The quantiles were obtained using the empirical distributions for each critical attribute.

For drive model 14, the central 99% empirical interval for the time between jumps in reallocated sector count, for hard drives that experience at least two jumps, is (23, 1360) h with a median of 24 h; the central 99% empirical interval for the size of the first jump in reallocated sector count, for drives with at least one nonzero jump, is (8, 34200) with a median of 72; and the central 99% empirical interval for the number of nonzero jumps in reallocated sector count, for drives that experienced at least one jump, is (1,176) with a median of 22 jumps.

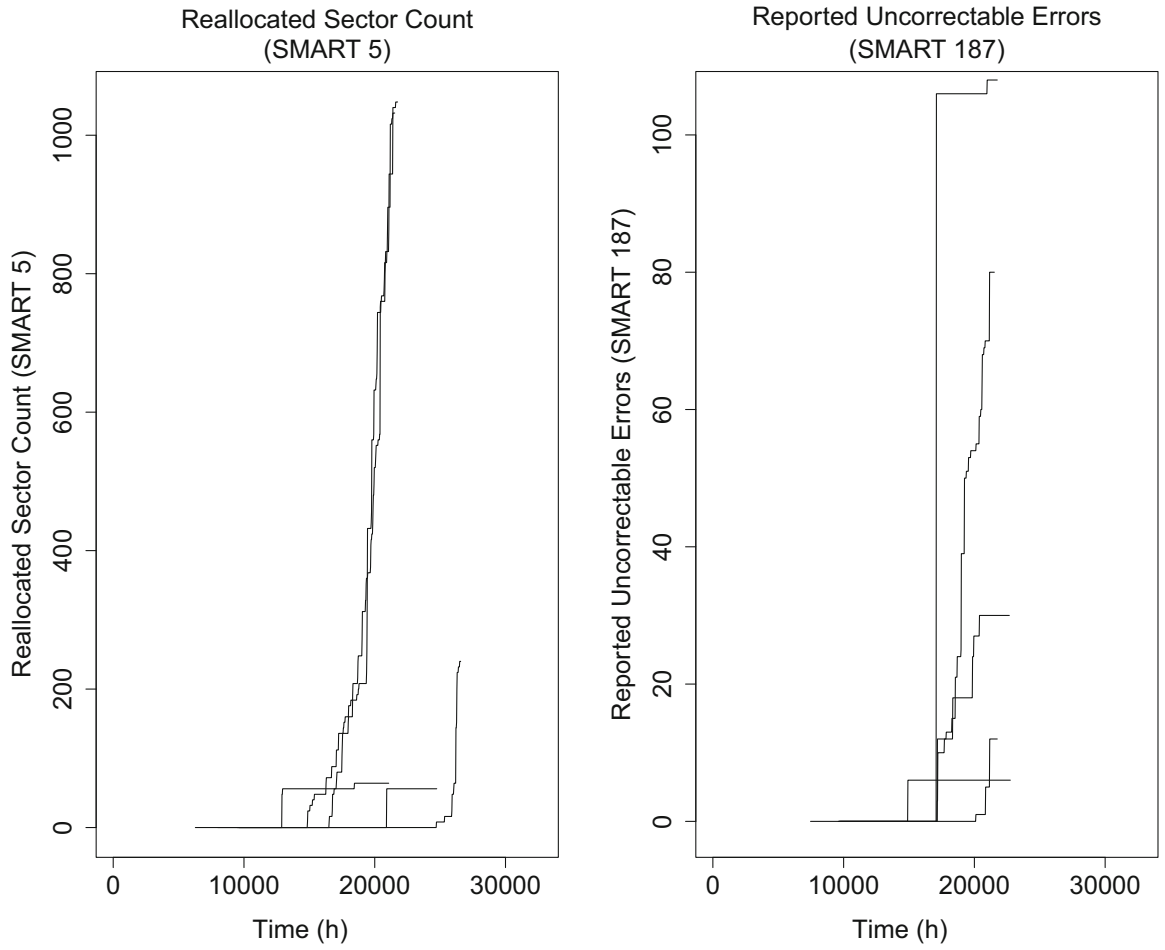


**FIGURE 3** Figure (left) depicts the longitudinal profile of the reallocated sector count (SMART 5) for five example hard drives. Figure (right) depicts the longitudinal profile of the reported uncorrectable errors (SMART 187) for five example hard drives.

**TABLE 1** Empirical distribution quantiles for the time between jumps, in hours, the size of each jump, and the number of nonzero jumps, for each critical attribute; alongside the proportion of drives with at least one and at least two jumps.

| | Time between jumps (h) | | | Size of jump | | | Number of nonzero jumps | | | Proportion of drives with at least | |
|---|---|---|---|---|---|---|---|---|---|---|---|
| **Critical attribute** | $\alpha_{0.005}$ | $\alpha_{0.5}$ | $\alpha_{0.995}$ | $\alpha_{0.005}$ | $\alpha_{0.5}$ | $\alpha_{0.995}$ | $\alpha_{0.005}$ | $\alpha_{0.5}$ | $\alpha_{0.995}$ | **1 jump** | **2 jumps** |
| SMART 5 | 23.0 | 24.0 | 1360 | 8.00 | 72.0 | 34200 | 1.00 | 22.0 | 176 | 0.253 | 0.239 |
| SMART 187 | 23.0 | 119.0 | 4310 | 1.00 | 6.00 | 432 | 1.00 | 2.00 | 39.7 | 0.368 | 0.236 |
| SMART 188 | 23.0 | 720 | 11800 | 1.00 | $4.72 \times 10^{10}$ | $2.10 \times 10^{11}$ | 1.00 | 2.00 | 18.3 | 0.840 | 0.557 |
| SMART 197 | 22.8 | 121 | 8890 | 8.00 | 8.00 | 65500 | 1.00 | 2.00 | 24.5 | 0.362 | 0.216 |
| SMART 198 | 23.0 | 120 | 3930 | 8.00 | 8.00 | 65500 | 1.00 | 2.00 | 22.5 | 0.275 | 0.159 |

Many hard drives do not experience a nonzero jump in reallocated sector count during their lifespan. More specifically, 75% of model 14 hard drives in our dataset do not experience a nonzero jump in reallocated sector count. For hard drives that experience a nonzero jump in reallocated sector count: some hard drives do not exhibit further jumps, some drives have frequent sporadic jumps thereafter, some of the subsequent jumps could be within days or thousands of hours later, and the size of the jumps vary drastically in size. Similar conclusions can be drawn from the other critical attributes. The erratic nature of these poorly understood processes makes it difficult to predict their values over time (with a "reasonable" amount of certainty that the predictions could be useful in a predictive model).

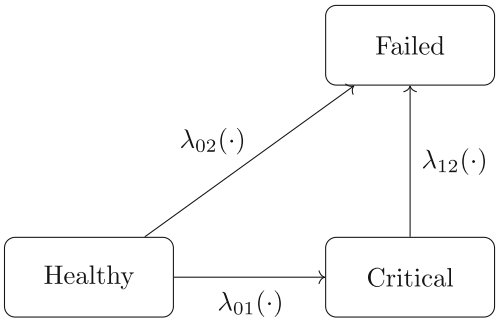


**FIGURE 4** An illness-death model where the critical state is defined as at least one critical attribute being nonzero.

We utilize the probabilities of changes in critical attributes and the age of a hard drive to predict the probability of drive failure over time. We treat changes in critical attributes as drives entering critical states. In this setting, the data collected by SMART can be considered semi-competing risks data. Under this definition of the critical states, we do not need to forecast the process for any critical attribute. Instead, we must forecast the probability of entering the critical states. It is difficult to predict the value of the critical attributes over time, but it is more manageable to obtain the probability of entering the critical states. In the next sections, we model the semi-competing risks data more formally using the illness-death model and the multistate model.

## 4.3 | Illness-death model

In this section, we model the semi-competing risks data using the illness-death model, where in our study of hard drives we take the terminal event to be failure, and the nonterminal event, the critical event, to be at least one critical attribute being nonzero. The illness-death model allows us to examine the impact of critical attributes on hard drive failure ages.

Let $T_1$ and $T_2$ denote critical and failure ages, respectively; where the critical age is defined as the age a drive enters the critical state, and the failure age is defined as the age a drive fails. We assume the convention of Xu et al.[17] and Lee et al.,[28] by setting $T_1 = \infty$ for drives which fail in the absence of the critical event. We assume an illness-death model for each individual drive of the form shown in Figure 4. The illness-death model is characterized by the transition hazards:

$$\lambda_{01}(t_1|\boldsymbol{\theta}_{01}) = \lim_{\Delta\to 0}\frac{\Pr(T_1 \in [t_1, t_1+\Delta)|T_1 \geq t_1, T_2 \geq t_1, \boldsymbol{\theta}_{01})}{\Delta}, \text{ for } t_1 > 0, \tag{6}$$

$$\lambda_{02}(t_2|\boldsymbol{\theta}_{02}) = \lim_{\Delta\to 0}\frac{\Pr(T_2 \in [t_2, t_2+\Delta)|T_1 \geq t_2, T_2 \geq t_2, \boldsymbol{\theta}_{02})}{\Delta}, \text{ for } t_2 > 0, \tag{7}$$

$$\lambda_{12}(t_2|T_1 = t_1, \boldsymbol{\theta}_{12}) = \lim_{\Delta\to 0}\frac{\Pr(T_2 \in [t_2, t_2+\Delta)|T_1 = t_1, T_2 \geq t_2, \boldsymbol{\theta}_{12})}{\Delta}, \text{ for } 0 < t_1 < t_2, \tag{8}$$

where $\lambda_{ij}$ is the hazard rate (transition intensity) of the $i \to j$ transition, $\boldsymbol{\theta}_{ij}$ is a vector of model parameters associated with $\lambda_{ij}$, and states 0, 1, and 2 correspond to the healthy, critical, and failed states, respectively.

### 4.3.1 | Observed data under the illness-death model

Let $T_{i1}$ and $T_{i2}$ denote the true critical and failure ages for drive $i$, respectively, and let $L_i$ and $C_i > L_i$ denote the left-truncation age and right-censoring age for drive $i$, respectively, which we assume are independent of $T_{i1}$ and $T_{i2}$. Moreover, let $Y_{i1} = \min(T_{i1}, T_{i2}, C_i)$ denote the observed critical age for drive $i$, with critical event indicator $\delta_{i1} = I\{T_{i1} \leq \min(T_{i2}, C_i)\}$, and let $Y_{i2} = \min(T_{i2}, C_i)$ denote the observed failure age for drive $i$, with failure indicator $\delta_{i2} = I\{T_{i2} \leq C_i\}$. The Backblaze hard drives are left-truncated and satisfy the recruitment criterion $L_i < Y_{i2}$. That is, hard drives that failed before the study commenced are not included in the dataset. The observed data for the $i$th drive is $D_i = \{l_i, y_{i1}, \delta_{i1}, y_{i2}, \delta_{i2}\}$.

Figure 5 provides a schematic representation of the six possible life histories observed under the illness-death model with left-truncation and right-censoring, alongside two descriptions of drives that are not included in the dataset since they do not satisfy the recruitment criterion, $L_i < Y_{i2}$. We illustrate the difference between event ages and event times

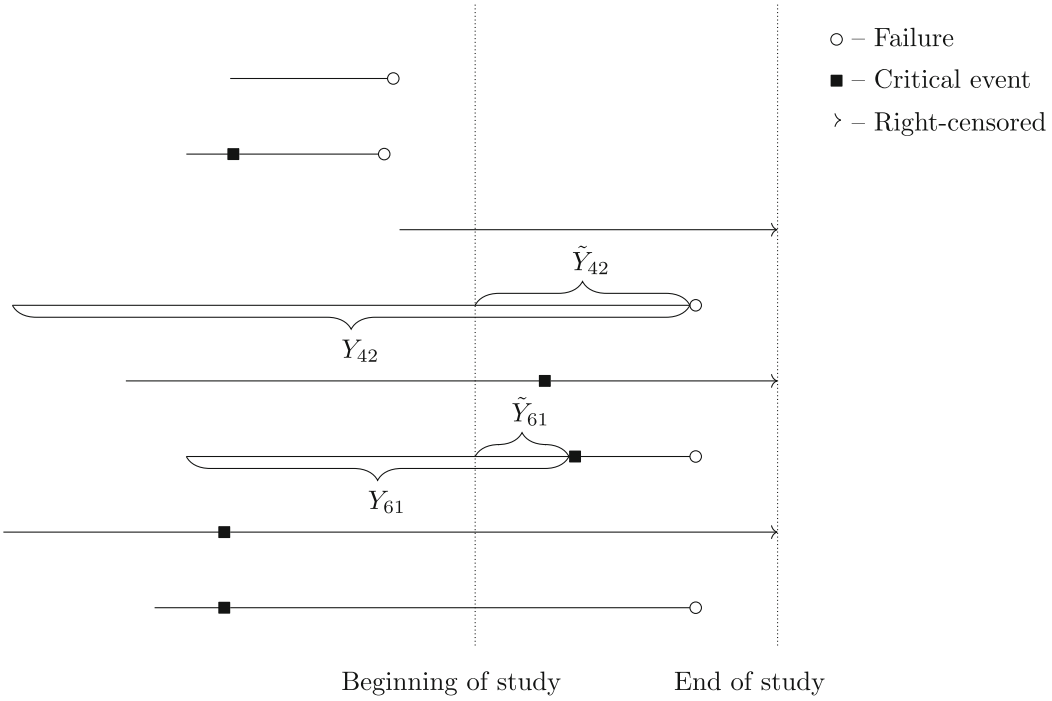


**FIGURE 5** Six possible life histories under the illness-death model and two example drives not included in the dataset.

using scenarios 4 and 6 in Figure 5. The failure age of drive 4 is denoted $Y_{42}$ and the failure time is denoted $\tilde{Y}_{42}$. The critical age of drive 6 is denoted $Y_{61}$ and the critical time is denoted $\tilde{Y}_{61}$. Drives 1 and 2 failed before the study began ($Y_{12} < L_1$, $Y_{22} < L_2$) and were not included in the dataset. Scenarios $3-8$ provide the six scenarios encountered under the illness-death model with left-truncation and right-censoring. Drive 3 was sampled in the healthy state ($L_3 < Y_{31}, Y_{32}$) and remained in the healthy state until the end of the study. Drive 3 is right-censored since it did not fail by the end of the study. Drive 4 was sampled in the healthy state ($L_4 < Y_{41}, Y_{42}$) and remained in the healthy state until failure ($T_{41} = \infty$). Drive 5 was sampled in the healthy state ($L_5 < Y_{51}, Y_{52}$) and transitioned to the critical state prior to the end of the study ($Y_{51} < Y_{52}$). Drive 5 is right-censored since it did not fail by the end of the study. Drive 6 was sampled in the healthy state ($L_6 < Y_{61}, Y_{62}$) and transitioned to the critical state prior to failure ($Y_{61} < Y_{62}$). Drives 7 and 8 were sampled in the critical state ($Y_{71} \leq L_7 < Y_{72}$, $Y_{81} \leq L_8 < Y_{82}$). Drive 7 is right-censored at the end of the study and drive 8 failed prior to the end of the study.

### 4.3.2 | Likelihood under the illness-death model

In this case the observed data take the form $\mathcal{D}_n = \{l_i, y_{i1}, \delta_{i1}, y_{i2}, \delta_{i2}; i = 1, \ldots, n\}$. Assuming the ages of the drives are independent, the censoring process is non-informative about $T_1$ and $T_2$, and that we do not have any knowledge about the truncation distribution, the likelihood for the data, $\mathcal{D}_n$, can be written as follows:

$$L(\boldsymbol{\theta}; \mathcal{D}_n) = \frac{L_{\text{Healthy}}(\boldsymbol{\theta}; \mathcal{D}_n) \times L_{\text{Critical}}(\boldsymbol{\theta}; \mathcal{D}_n)}{L_{\text{Truncation}}(\boldsymbol{\theta}; \mathcal{D}_n)}, \tag{9}$$

as described in;[29] where $\boldsymbol{\theta} = (\boldsymbol{\theta}_{01}, \boldsymbol{\theta}_{02}, \boldsymbol{\theta}_{12})$ is a vector of model parameters,

$$\begin{aligned} L_{\text{Healthy}}(\boldsymbol{\theta}; \mathcal{D}_n) = \prod_{i: l_i < y_{i1}, y_{i2}} & \left[ S_{01}(y_{i2}|\boldsymbol{\theta}_{01}) S_{02}(y_{i2}|\boldsymbol{\theta}_{02}) \lambda_{02}^{\delta_{i2}}(y_{i2}|\boldsymbol{\theta}_{02}) \right]^{1-\delta_{i1}} \\ & \times \left[ S_{01}(y_{i1}|\boldsymbol{\theta}_{01}) S_{02}(y_{i1}|\boldsymbol{\theta}_{02}) \lambda_{01}(y_{i1}|\boldsymbol{\theta}_{01}) S_{12}(y_{i2}|y_{i1}, \boldsymbol{\theta}_{12}) \lambda_{12}^{\delta_{i2}}(y_{i2}|y_{i1}, \boldsymbol{\theta}_{12}) \right]^{\delta_{i1}}, \end{aligned} \tag{10}$$

is the contribution to the likelihood from drives sampled in the healthy state,

$$L_{\text{Critical}}(\boldsymbol{\theta};\mathcal{D}_n)=\prod_{i:y_{i1}\le l_i<y_{i2}}\int_0^{l_i}\left[S_{01}(t|\boldsymbol{\theta}_{01})S_{02}(t|\boldsymbol{\theta}_{02})\lambda_{01}(t|\boldsymbol{\theta}_{01})S_{12}(y_{i2}|t,\boldsymbol{\theta}_{12})\lambda_{12}^{\delta_{i2}}(y_{i2}|t,\boldsymbol{\theta}_{12})\right]^{\delta_{i1}}dt, \tag{11}$$

is the contribution to the likelihood from drives sampled in the critical state, and

$$L_{\text{Truncation}}(\boldsymbol{\theta};\mathcal{D}_n)=\prod_i\left\{S_{01}(l_i|\boldsymbol{\theta}_{01})S_{02}(l_i|\boldsymbol{\theta}_{02})+\int_0^{l_i}S_{01}(t|\boldsymbol{\theta}_{01})S_{02}(t|\boldsymbol{\theta}_{02})\lambda_{01}(t|\boldsymbol{\theta}_{01})S_{12}(l_i|t,\boldsymbol{\theta}_{12})dt\right\}, \tag{12}$$

is the likelihood of survival up to the sampling age. In addition, $S_{0k}(t|\boldsymbol{\theta}_{0k})=\exp\left(-\int_0^t\lambda_{0k}(u|\boldsymbol{\theta}_{0k})du\right)$, for $k=1,2$, is the probability that drive $i$ does not transition from $0\to k$ by age $t$; and $S_{12}(t_2|t_1,\boldsymbol{\theta}_{12})=\exp\left(-\int_{t_1}^{t_2}\lambda_{12}(u|\boldsymbol{\theta}_{12})du\right)$ is the probability that drive $i$ does not transition from $1\to 2$ by age $t_2$ given that drive $i$ is in the critical state at age $t_1$.

The first term in Equation (10) is the likelihood contribution from a drive that is sampled in the healthy state and does not transition to the critical state (see scenarios 3 and 4 in Figure 5). In other words, this contribution is the likelihood of staying in the healthy state up until age $y_{i2}$, for right-censored drives, and then moving from the healthy state to the failed state, at age $y_{i2}$, for drives that failed. The second term in Equation (10) is the likelihood contribution from a drive that is sampled in the healthy state and transitions to the critical state prior to the end of the study or failure (see scenarios 5 and 6 in Figure 5). In other words, this contribution is the likelihood of staying in the healthy state up until age $y_{i1}$, transitioning to the critical state at $y_{i1}$, and remaining in the critical state until age $y_{i2}$, for right-censored drives, and moving from the critical state to the failed state, at age $y_{i2}$, for drives that failed.

Equation (11) is the likelihood contribution from drives that are sampled in the critical state (see scenarios 7 and 8 in Figure 5). For these drives, we know they transitioned to the critical state at age $y_{i1}\le l_i<y_{i2}$ and remained in the critical state until the end of the study if right-censored, or until failure for drives that failed. The integrand is identical to the second term in Equation (10), however, for drives sampled in the critical state, we need to integrate over all possible transition ages.

Equation (12) is the likelihood of survival up to the sampling age. We need to calculate the probability of survival up to the sampling age, $l_i$, for each drive. This probability is a sum of two terms: the probability of being sampled in the healthy state (term 1), and the probability of being sampled in the critical state (term 2).

### 4.3.3 | Posterior predictive survival distributions under the illness-death model

Let $z_i(\gamma)$ represent the state of drive $i$ at age $\gamma$. Drive $i$ is either in the healthy state, $\{0\}$, the critical state, $\{1\}$, or the failed state, $\{2\}$. Under the illness-death model, the posterior predictive survival distributions are given by:

$$\Pr(T\ge\gamma+s|T>\gamma,z(\gamma),\mathcal{D}_n)=\int\Pr(T\ge\gamma+s|T>\gamma,z(\gamma),\boldsymbol{\theta})p(\boldsymbol{\theta}|\mathcal{D}_n)d\boldsymbol{\theta}, \tag{13}$$

for $z_i(\gamma)=0,1$, where

$$\begin{aligned}&\Pr(T_2\ge\gamma+s|T_2>\gamma,z(\gamma)=0,\boldsymbol{\theta}_{01},\boldsymbol{\theta}_{02},\boldsymbol{\theta}_{12})\\&\quad=\frac{1}{S_{01}(\gamma|\boldsymbol{\theta}_{01})S_{02}(\gamma|\boldsymbol{\theta}_{02})}\left\{S_{01}(\gamma+s|\boldsymbol{\theta}_{01})S_{02}(\gamma+s|\boldsymbol{\theta}_{02})+\int_\gamma^{\gamma+s}S_{01}(\nu|\boldsymbol{\theta}_{01})S_{02}(\nu|\boldsymbol{\theta}_{02})\lambda_{01}(\nu|\boldsymbol{\theta}_{01})S_{12}(\gamma+s|\nu,\boldsymbol{\theta}_{12})d\nu\right\},\end{aligned} \tag{14}$$

for drives in the healthy state at age $\gamma$, and

$$\Pr(T_2\ge\gamma+s|T_2>\gamma,z(\gamma)=1,\boldsymbol{\theta}_{12})=S_{12}(\gamma+s|\gamma,\boldsymbol{\theta}_{12}), \tag{15}$$

for drives in the critical state at age $\gamma$. In Equation (14), the first term represents the probability the drive remained in the healthy state from age $\gamma$ to $\gamma+s$, and the second term is the probability the drive transitioned from the healthy state to the critical state at age $\nu\in(\gamma,\gamma+s)$ and then remained in the critical state from age $\nu$ to $\gamma+s$, integrated over $\nu$.

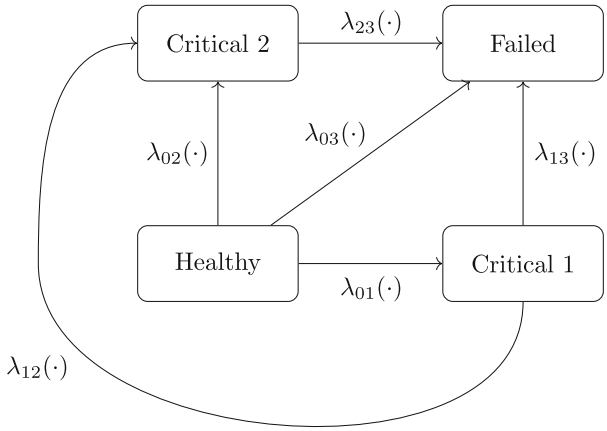


**FIGURE 6** A multistate model where the critical 1 state is defined as one critical attribute being nonzero and the critical 2 state is defined as at least two critical attributes being nonzero.

In addition,

$$p(\boldsymbol{\theta}|\mathcal{D}_n) \tag{16}$$

is the posterior distribution of the illness-death model parameters given the observed data, $\mathcal{D}_n$.

## 4.4 | Multistate model

A multistate model is used to model a process where drives transition from one state to the next. For instance, the two-state model, proposed in Section 3, is a simple multistate model with two states (healthy and failed) with one transition between those two states (see Figure 1). The illness-death model, proposed in Section 4.3, is a multistate model with three states (healthy, critical, and failed, see Figure 4). Figure 6 depicts a multistate model with four states: namely, the healthy state (state 0), the critical 1 state (state 1), the critical 2 state (state 2), and the failed state (state 3).

In this section, we outline how to model the semi-competing risks data using a four-state multistate model, referred to as the multistate model, where in our study of hard drives we take the terminal event to be failure, and the nonterminal events, the critical 1 and critical 2 events, to be one critical attribute being nonzero, and at least two critical attributes being nonzero, respectively. This multistate model will allow us to examine the impact of a single critical attribute and the impact of multiple critical attributes on hard drive failure ages.

Let $T_1$, $T_2$ and $T_3$ denote critical 1, critical 2 and failure ages, respectively; where the critical $j$ age, for $j = 1, 2$, is defined as the age a drive enters state $j$, and the failure age is defined as the age a drive fails. We assume $T_1 = T_2 = \infty$ for drives which fail in the absence of the critical events. We assume a multistate model for each individual drive of the form shown in Figure 6. Following the approach from Section 4.3, the multistate model is characterized by the transition hazards:

$$\lambda_{01}(t_1|\boldsymbol{\theta}_{01}) = \lim_{\Delta\to 0}\frac{\Pr(T_1 \in [t_1, t_1+\Delta)|T_1 \geq t_1, T_2 \geq t_1, T_3 \geq t_1, \boldsymbol{\theta}_{01})}{\Delta}, \text{ for } t_1 > 0, \tag{17}$$

$$\lambda_{02}(t_2|\boldsymbol{\theta}_{02}) = \lim_{\Delta\to 0}\frac{\Pr(T_2 \in [t_2, t_2+\Delta)|T_1 \geq t_2, T_2 \geq t_2, T_3 \geq t_2, \boldsymbol{\theta}_{02})}{\Delta}, \text{ for } t_2 > 0, \tag{18}$$

$$\lambda_{03}(t_3|\boldsymbol{\theta}_{03}) = \lim_{\Delta\to 0}\frac{\Pr(T_3 \in [t_3, t_3+\Delta)|T_1 \geq t_3, T_2 \geq t_3, T_3 \geq t_3, \boldsymbol{\theta}_{03})}{\Delta}, \text{ for } t_3 > 0, \tag{19}$$

$$\lambda_{12}(t_2|T_1 = t_1, \boldsymbol{\theta}_{12}) = \lim_{\Delta\to 0}\frac{\Pr(T_2 \in [t_2, t_2+\Delta)|T_1 = t_1, T_2 \geq t_2, T_3 \geq t_2, \boldsymbol{\theta}_{12})}{\Delta}, \text{ for } 0 < t_1 < t_2, \tag{20}$$

$$\lambda_{13}(t_3|T_1 = t_1, \boldsymbol{\theta}_{13}) = \lim_{\Delta\to 0}\frac{\Pr(T_3 \in [t_3, t_3+\Delta)|T_1 = t_1, T_2 \geq t_3, T_3 \geq t_3, \boldsymbol{\theta}_{13})}{\Delta}, \text{ for } 0 < t_1 < t_3, \tag{21}$$

$$\lambda_{23}(t_3|T_2 = t_2, \boldsymbol{\theta}_{23}) = \lim_{\Delta\to 0}\frac{\Pr(T_3 \in [t_3, t_3+\Delta)|T_2 = t_2, T_3 \geq t_3, \boldsymbol{\theta}_{23})}{\Delta}, \text{ for } 0 < t_2 < t_3, \tag{22}$$

where $\lambda_{ij}$ is the hazard rate (transition intensity) of the $i \to j$ transition, $\boldsymbol{\theta}_{ij}$ is a vector of model parameters associated with $\lambda_{ij}$, and states 0, 1, 2, and 3 correspond to the healthy, critical 1, critical 2, and failed states, respectively.

In Section C in the supplementary material we describe the data observed, derive the likelihood for hard drives subject to left-truncation and right-censoring, and propose the posterior predictive survival distributions for working drives, under the multistate model.

## 5 | MEASURING PREDICTIVE PERFORMANCE

To assess the performance of dynamic predictions, we use calibration, i.e., how well a model predicts failures,[32,33] and discrimination, i.e., how well a model can discriminate between drives that fail and drives that do not fail,[34,35] measures. We use the time-dependent area under the receiver operating characteristic curve (AUC),[36] as a discriminative measure, to compare how well the two-state model, the illness-death model, and the multistate model can discriminate between drives that fail and drives that do not fail. We use the expected prediction error (PE),[36,37] as a measure of model calibration, to compare how well each model can predict hard drive failure ages.

In this section, we first describe the AUC and the PE under the illness-death model. Then, we provide adaptions for the two-state model and the multistate model. We assume an illness-death model for each individual drive of the form shown in Figure 4.

Define the survival probability

$$\rho_i(\tau_i + s|\tau_i, z(\tau_i), \mathcal{D}_n) = \begin{cases} \Pr(T_{i2} \geq \tau_i + s | T_{i2} > \tau_i, z(\tau_i) = 0, \mathcal{D}_n), \\ \text{if drive } i \text{ is in the healthy state at age } \tau_i, \\ \Pr(T_{i2} \geq \tau_i + s | T_{i2} > \tau_i, z(\tau_i) = 1, \mathcal{D}_n), \\ \text{if drive } i \text{ is in the critical state at age } \tau_i, \end{cases} \tag{23}$$

where $\tau_i$ is the age of drive $i$ at time $\tau$, $z(\tau_i)$ is the state of drive $i$ at age $\tau_i$, $\tau \geq 0$ is the time elapsed since the beginning of the study, $s > 0$ is the forecast horizon of interest, $T_{i2}$ is the true failure age of drive $i$, $\mathcal{D}_n$ is the observed data used to obtain the posterior distribution of the illness-death model parameters, and the relevant expressions are given in Equations (14) and (15), respectively. The time elapsed since the beginning of the study, $\tau$, will be referred to as the calendar time from herein. The quantity $\rho_i(\tau_i + s|\tau_i, z(\tau_i), \mathcal{D}_n)$ is the probability that drive $i$ does not fail by age $\tau_i + s$ conditional on being in a working state (i.e., not in the failed state) at age $\tau_i$. In other words, the quantity $\rho_i(\tau_i + s|\tau_i, z(\tau_i), \mathcal{D}_n)$ is the probability that drive $i$ does not fail by calendar time $\tau + s$ conditional on being in a working state at calendar time $\tau$.

### 5.1 | Time-dependent area under the receiver operating characteristic curve (AUC)

The AUC is a measure of discrimination of a model. At calendar time $\tau$, drive $i$ is defined as a case if $\tilde{T}_{i2} \in (\tau, \tau + s]$ and a control if $\tilde{T}_{i2} > \tau + s$, where $\tilde{T}_{i2}$ is the true failure time of drive $i$. In other words, drive $i$ is a case if it fails within the forecast horizon $(\tau, \tau + s]$ and a control if it survives the forecast horizon. The AUC measures our model's ability to distinguish between a case and a control. Following Rizopoulos et al.,[36] consider at calendar time $\tau$ a pair of randomly chosen hard drives, $(i, j)$, for which drive $i$ is a case and drive $j$ is a control. The AUC is given by

$$\text{AUC}(\tau, s) = \Pr\left[\rho_i(\tau_i + s|\tau_i, z(\tau_i), \mathcal{D}_n) < \rho_j(\tau_j + s|\tau_j, z(\tau_j), \mathcal{D}_n) | \{\tilde{T}_{i2} \in (\tau, \tau + s]\} \cap \{\tilde{T}_{j2} > \tau + s\}\right], \tag{24}$$

where $\tilde{T}_{i2}$ and $\tilde{T}_{j2}$ are the failure times for drives $i$ and $j$, respectively, and $T_{i2}$ and $T_{j2}$ are the failure ages for drives $i$ and $j$, respectively.

If drive $i$ fails within the forecast horizon and drive $j$ is in a working state after the forecast horizon, then we would expect the assumed model to provide a higher probability of surviving the forecast horizon to the hard drive that survives (hard drive $j$) compared to the hard drive that fails (hard drive $i$).

If there are no right-censored failure ages within the forecast horizon, then the AUC can be estimated by

$$\hat{\text{AUC}}(\tau, s) = \frac{1}{n_{\text{fail}}(\tau) n_{\text{surv}}(\tau)} \sum_{i=1}^{n_{\text{fail}}(\tau)} \sum_{j=1}^{n_{\text{surv}}(\tau)} \mathbb{E}_{\rho_i(\cdot), \rho_j(\cdot)} \left[ I\left\{ \rho_i(\tau_i + s|\tau_i, z(\tau_i), \mathcal{D}_n) < \rho_j(\tau_j + s|\tau_j, z(\tau_j), \mathcal{D}_n) \right\} \right], \tag{25}$$

where $n_{\text{fail}}(\tau)$ is the number of drives that fail within the forecast horizon $(\tau, \tau + s]$ and $n_{\text{surv}}(\tau)$ is the number of drives that survive the forecast horizon and the expectation is taken with respect to the posterior predictive distributions of $\rho_i(\tau_i + s|\tau_i, z(\tau_i), \mathcal{D}_n)$ and $\rho_j(\tau_j + s|\tau_j, z(\tau_j), \mathcal{D}_n)$. If $\hat{\text{AUC}}(\tau, s) = 1$, then our model always gives a higher probability of surviving to drives that survive compared to drives that fail.

Since many hard drive failure ages are right-censored within the forecast horizon, estimation of the AUC is based on counting the concordant pairs of drives by appropriately distinguishing between the comparable and the "partially comparable" (due to censoring) pairs of drives at calendar time $\tau$. More specifically, the pairs of drives that are comparable are given by the set

$$\Omega_{ij}^{(1)}(\tau, s) = \left[\{\tilde{Y}_{i2} \in (\tau, \tau + s]\} \cap \{\delta_{i2} = 1\}\right] \cap \{\tilde{Y}_{j2} > \tau + s\}, \tag{26}$$

for $i, j = 1, \ldots, n(\tau)$, with $i \neq j$, $n(\tau)$ is the number of drives in a working state at calendar time $\tau$, and $\tilde{Y}_{i2}$ and $\tilde{Y}_{j2}$ are the observed failure times for drives $i$ and $j$, respectively. In words, $\Omega_{ij}^{(1)}(\tau, s)$, for $i, j = 1, \ldots, n(\tau)$, with $i \neq j$, is the set of all pairs of drives, such that drive $i$ is observed to fail within the forecast horizon (a case), and drive $j$ is observed to survive the forecast horizon (a control). The remaining pairs of drives which, due to censoring, cannot be directly compared, are given by the following sets:

$$\begin{aligned}
\Omega_{ij}^{(2)}(\tau, s) &= \left[\{\tilde{Y}_{i2} \in (\tau, \tau + s]\} \cap \{\delta_{i2} = 0\}\right] \cap \{\tilde{Y}_{j2} > \tau + s\}, \\
\Omega_{ij}^{(3)}(\tau, s) &= \left[\{\tilde{Y}_{i2} \in (\tau, \tau + s]\} \cap \{\delta_{i2} = 1\}\right] \cap \left[\{\tilde{Y}_{i2} < \tilde{Y}_{j2} \leq \tau + s\} \cap \{\delta_{j2} = 0\}\right], \\
\Omega_{ij}^{(4)}(\tau, s) &= \left[\{\tilde{Y}_{i2} \in (\tau, \tau + s]\} \cap \{\delta_{i2} = 0\}\right] \cap \left[\{\tilde{Y}_{i2} < \tilde{Y}_{j2} \leq \tau + s\} \cap \{\delta_{j2} = 0\}\right].
\end{aligned} \tag{27}$$

In order for a pair of drives $(i, j)$ to be directly comparable, drive $i$ must be observed to fail within the forecast horizon and drive $j$ must be observed to survive the forecast horizon; we need a case and a control.

The failure time of drive $i$ in $\Omega_{ij}^{(2)}(\tau, s)$ is right-censored. Since the true failure time of drive $i$ is not observed, we do not know if drive $i$ fails within the forecast horizon or not. Thus, drives in $\Omega_{ij}^{(2)}(\tau, s)$ are not directly comparable since we cannot directly identify a case and a control. Similarly, the failure time for drive $j$ in $\Omega_{ij}^{(3)}(\tau, s)$ is right-censored such that $\tilde{Y}_{i2} < \tilde{Y}_{j2} \leq \tau + s$. Therefore, we do not know if drive $j$ survives the forecast horizon. Thus, drives in $\Omega_{ij}^{(3)}(\tau, s)$ are not directly comparable. Finally, the failure times of both drives in $\Omega_{ij}^{(4)}(\tau, s)$ are right-censored, such that $\tilde{Y}_{i2} < \tilde{Y}_{j2} \leq \tau + s$. Thus, drives in $\Omega_{ij}^{(4)}(\tau, s)$ are not directly comparable.

The partially comparable drives contribute to the overall AUC after being appropriately weighted with the probability of being comparable

$$\begin{aligned}
\nu_i^{(2)}(\tau, s|Y_{i2}, z(Y_{i2}), \mathcal{D}_n) &= 1 - \rho_i(\tau_i + s|Y_{i2}, z(Y_{i2}), \mathcal{D}_n), \\
\nu_j^{(3)}(\tau, s|Y_{j2}, z(Y_{j2}), \mathcal{D}_n) &= \rho_j(\tau_j + s|Y_{j2}, z(Y_{j2}), \mathcal{D}_n), \\
\nu_{ij}^{(4)}(\tau, s|Y_{i2}, z(Y_{i2}), Y_{j2}, z(Y_{j2}), \mathcal{D}_n) &= (1 - \rho_i(\tau_i + s|Y_{i2}, z(Y_{i2}), \mathcal{D}_n)) \times \rho_j(\tau_j + s|Y_{j2}, z(Y_{j2}), \mathcal{D}_n),
\end{aligned} \tag{28}$$

where $Y_{i2}$ and $Y_{j2}$ are the observed failure ages for drives $i$ and $j$, respectively. In words, $\nu_i^{(2)}(\tau, s|Y_{i2}, z(Y_{i2}), \mathcal{D}_n)$ is the probability drive $i$ fails within the forecast horizon, conditional on surviving until age $Y_{i2}$. In other words, $\nu_i^{(2)}(\tau, s|Y_{i2}, z(Y_{i2}), \mathcal{D}_n)$ is the probability that a pair of drives in $\Omega_{ij}^{(2)}(\tau, s)$ is comparable. Similarly, $\nu_j^{(3)}(\tau, s|Y_{j2}, z(Y_{j2}), \mathcal{D}_n)$ is the probability that drive $j$ survives the forecast horizon, conditional on surviving until age $Y_{j2}$. In other words, $\nu_j^{(3)}(\tau, s|Y_{j2}, z(Y_{j2}), \mathcal{D}_n)$ is the probability that a pair of drives in $\Omega_{ij}^{(3)}(\tau, s)$ is comparable. Finally, $\nu_{ij}^{(4)}(\tau, s|Y_{i2}, z(Y_{i2}), Y_{j2}, z(Y_{j2}), \mathcal{D}_n)$ is the probability that drive $i$ fails within the forecast horizon, conditional on surviving until age $Y_{i2}$, and drive $j$ survives the forecast horizon, conditional on surviving until age $Y_{j2}$. In other words, $\nu_{ij}^{(4)}(\tau, s|Y_{i2}, z(Y_{i2}), Y_{j2}, z(Y_{j2}), \mathcal{D}_n)$ is the probability that a pair of drives in $\Omega_{ij}^{(4)}(\tau, s)$ is comparable.

The time-dependent area under the receiver operating characteristic curve at time $\tau$, as proposed by Rizopoulos et al.,[36] is given by

$$\hat{\text{AUC}}(\tau, s) = \frac{\kappa_1(\tau, s) + \kappa_2(\tau, s) + \kappa_3(\tau, s) + \kappa_4(\tau, s)}{\zeta_1(\tau, s) + \zeta_2(\tau, s) + \zeta_3(\tau, s) + \zeta_4(\tau, s)}, \tag{29}$$

where

$$\kappa_1(\tau,s)=\sum_{i=1}^{n(\tau)}\sum_{j=1,j\neq i}^{n(\tau)}\mathbb{E}_{\rho_i(\cdot),\rho_j(\cdot)}\left[I\left\{\rho_i(\tau_i+s|\tau_i,z(\tau_i),\mathcal{D}_n)<\rho_j(\tau_j+s|\tau_j,z(\tau_j),\mathcal{D}_n)\right\}\right]I\{\Omega_{ij}^{(1)}(\tau,s)\},$$

$$\kappa_2(\tau,s)=\sum_{i=1}^{n(\tau)}\sum_{j=1,j\neq i}^{n(\tau)}\mathbb{E}_{\rho_i(\cdot),\rho_j(\cdot)}\left[I\left\{\rho_i(\tau_i+s|\tau_i,z(\tau_i),\mathcal{D}_n)<\rho_j(\tau_j+s|\tau_j,z(\tau_j),\mathcal{D}_n)\right\}\right]I\{\Omega_{ij}^{(2)}(\tau,s)\}\nu_i^{(2)},$$

$$\kappa_3(\tau,s)=\sum_{i=1}^{n(\tau)}\sum_{j=1,j\neq i}^{n(\tau)}\mathbb{E}_{\rho_i(\cdot),\rho_j(\cdot)}\left[I\left\{\rho_i(\tau_i+s|\tau_i,z(\tau_i),\mathcal{D}_n)<\rho_j(\tau_j+s|\tau_j,z(\tau_j),\mathcal{D}_n)\right\}\right]I\{\Omega_{ij}^{(3)}(\tau,s)\}\nu_j^{(3)},$$

$$\kappa_4(\tau,s)=\sum_{i=1}^{n(\tau)}\sum_{j=1,j\neq i}^{n(\tau)}\mathbb{E}_{\rho_i(\cdot),\rho_j(\cdot)}\left[I\left\{\rho_i(\tau_i+s|\tau_i,z(\tau_i),\mathcal{D}_n)<\rho_j(\tau_j+s|\tau_j,z(\tau_j),\mathcal{D}_n)\right\}\right]I\{\Omega_{ij}^{(4)}(\tau,s)\}\nu_{ij}^{(4)}, \tag{30}$$

and

$$\zeta_1(\tau,s)=\sum_{i=1}^{n(\tau)}\sum_{j=1,j\neq i}^{n(\tau)}I\{\Omega_{ij}^{(1)}(\tau,s)\},$$

$$\zeta_2(\tau,s)=\sum_{i=1}^{n(\tau)}\sum_{j=1,j\neq i}^{n(\tau)}I\{\Omega_{ij}^{(2)}(\tau,s)\}\nu_i^{(2)},$$

$$\zeta_3(\tau,s)=\sum_{i=1}^{n(\tau)}\sum_{j=1,j\neq i}^{n(\tau)}I\{\Omega_{ij}^{(3)}(\tau,s)\}\nu_j^{(3)},$$

$$\zeta_4(\tau,s)=\sum_{i=1}^{n(\tau)}\sum_{j=1,j\neq i}^{n(\tau)}I\{\Omega_{ij}^{(4)}(\tau,s)\}\nu_{ij}^{(4)}. \tag{31}$$

In addition, $I_A$ is an indicator function, which is equal to 1 if event $A$ occurs and 0 otherwise.

For all pairs of drives $(i,j)$ in the set $\Omega_{ij}^{(1)}(\tau,s)$, $\kappa_1(\tau,s)$ is the number of times the illness-death model gives the control a higher probability of surviving the forecast horizon compared to the case. Moreover, $\zeta_1(\tau,s)$ is the number of pairs of drives in the set $\Omega_{ij}^{(1)}(\tau,s)$. If all pairs of drives were comparable, that is, if all pairs of drives were contained in the set $\Omega_{ij}^{(1)}(\tau,s)$, then Equation (29) reduces to

$$\hat{\text{AUC}}(\tau,s)=\frac{\kappa_1(\tau,s)}{\sum_{i=1}^{n(\tau)}\sum_{j=1,j\neq i}^{n(\tau)}I\left\{\Omega_{ij}^{(1)}(\tau,s)\right\}}, \tag{32}$$

which is equivalent to Equation (25).

Similar definitions can be made for $\kappa_l(\tau,s)$ and $\zeta_l(\tau,s)$, for $l=2,3,4$, but each term in $\kappa_l(\tau,s)$ and $\zeta_l(\tau,s)$, for $l=2,3,4$, is weighted by the probability of the pair of drives, $(i,j)$, being comparable, that is, the probability that drive $i$ fails within the forecast horizon and drive $j$ survives the forecast horizon. $\hat{\text{AUC}}(\tau,s)$, given by Equation (29), accounts for right-censored observations in the forecast horizon, and is interpreted as the probability the illness-death model gives the control a higher probability of surviving the forecast horizon compared to the case.

## 5.2 | Time-dependent expected predicted error (PE)

The expected predicted error in predicting future failures can be used to assess the accuracy of dynamic predictions.[36] As for the AUC we focus our interest in predicting failures that occur by calendar time $\tau+s>\tau$ given the information available up to calendar time $\tau$. The expected predicted error for a working drive at time $\tau$ is given by

$$\text{PE}(\tau+s|\tau)=\mathbb{E}_{\rho_i(\cdot)}\left[\mathbb{E}_{T_{i2}}\left[L\{N_i(\tau+s)-\rho_i(\tau_i+s|\tau_i,z(\tau_i),\mathcal{D}_n)\}\right]\right], \tag{33}$$

where $N_i(\tau+s)=I(T_{i2}>\tau_i+s)=I(\tilde{T}_{i2}>\tau+s)$ denotes the survival status of hard drive $i$ at calendar time $\tau+s$, where $N_i(\tau+s)=1$ if hard drive $i$ survives the forecast horizon and $N_i(\tau+s)=0$ if hard drive $i$ fails within the forecast horizon;

$L(\cdot)$ denotes a loss function, such as the absolute or square loss; the inner expectation is taken with respect to the posterior predictive distribution of $T_{i2}$ and the outer expectation is taken with respect to the posterior predictive distribution of $\rho_i(\tau_i + s|\tau_i, z(\tau_i), \mathcal{D}_n)$.

The PE is a calibration measure that measures how well a model predicts failures. The smaller the value of $N_i(\tau + s) - \rho_i(\tau_i + s|\tau_i, z(\tau_i), \mathcal{D}_n)$, the smaller the PE, or the more accurate the model is. That is, for drives that survive, the closer $\rho_i(\tau_i + s|\tau_i, z(\tau_i), \mathcal{D}_n)$ is to 1 (i.e., the higher the probability of survival), the smaller $N_i(\tau + s) - \rho_i(\tau_i + s|\tau_i, z(\tau_i), \mathcal{D}_n)$ will be. We want our model to give a high probability of surviving the forecast horizon of interest to drives that survive. In contrast, we want our model to give a low probability of surviving the forecast horizon to drives that fail within the forecast horizon. For drives that fail, the closer $\rho_i(\tau_i + s|\tau_i, z(\tau_i), \mathcal{D}_n)$ is to 0 (i.e., the lower the survival probability), the smaller $N_i(\tau + s) - \rho_i(\tau_i + s|\tau_i, z(\tau_i), \mathcal{D}_n)$ will be. An accurate model will give high probabilities of surviving to drives that survive and low probabilities of surviving to drives that fail.

An estimate of $\text{PE}(\tau + s|\tau)$ that accounts for censoring has been proposed by Henderson et al.[37] and is given by

$$\begin{aligned}
\hat{\text{PE}}(\tau + s|\tau) = \frac{1}{n(\tau)} \sum_{i=1}^{n(\tau)} & I\{\tilde{Y}_{i2} > \tau + s\} \mathbb{E}_{\rho_i(\cdot)}\left[L(1 - \rho_i(\tau_i + s|\tau_i, z(\tau_i), \mathcal{D}_n))\right] \\
& + \delta_i I\{\tilde{Y}_{i2} < \tau + s\} \mathbb{E}_{\rho_i(\cdot)}\left[L(0 - \rho_i(\tau_i + s|\tau_i, z(\tau_i), \mathcal{D}_n))\right] \\
& + (1 - \delta_i) I\{\tilde{Y}_{i2} < \tau + s\} \Big\{ \mathbb{E}_{\rho_i(\cdot)}\left[\rho_i(\tau_i + s|Y_{i2}, z(Y_{i2}), \mathcal{D}_n)\right] \mathbb{E}_{\rho_i(\cdot)}\left[L(1 - \rho_i(\tau_i + s|\tau_i, z(\tau_i), \mathcal{D}_n))\right] \\
& + \left(1 - \mathbb{E}_{\rho_i(\cdot)}\left[\rho_i(\tau_i + s|Y_{i2}, z(Y_{i2}), \mathcal{D}_n)\right]\right) \mathbb{E}_{\rho_i(\cdot)}\left[L(0 - \rho_i(\tau_i + s|\tau_i, z(\tau_i), \mathcal{D}_n))\right] \Big\},
\end{aligned} \tag{34}$$

where $n(\tau)$ denotes the number of hard drives that are in a working state at calendar time $\tau$. The first term in Equation (34) is the contribution from a drive that is in a working state after time $\tau + s$, in other words, the contribution from a drive that survives the forecast horizon; the second term is the contribution from a drive that fails within the forecast horizon; the third and fourth terms are the contributions from a drive that is censored in the forecast horizon $(\tau, \tau + s)$. Using the information up to time $\tau$, $\text{PE}(\tau + s|\tau)$ measures the predictive accuracy at calendar time $\tau$.

## 5.3 | Adaptions for the two-state model and the multistate model

In this section we have described the AUC and the PE under the illness-death model shown in Figure 4. The definitions of the AUC and the PE can be adapted for the two-state model, shown in Figure 1, and the multistate model, shown in Figure 6.

Under the two-state model we define

$$\rho_i(\tau_i + s|\tau_i, \mathcal{D}_n) = \Pr(T_i \geq \tau_i + s|T_i > \tau_i, \mathcal{D}_n), \tag{35}$$

where $\tau_i$ is the age of drive $i$ at time $\tau$, $T_i$ is the true failure age of drive $i$, $\mathcal{D}_n$ is the observed data used to obtain the posterior distribution of the two-state model parameters, and the relevant expression is given in Equation (3). Under the two-state model, in the definitions of the AUC and the PE, given in Sections 5.1 and 5.2, respectively, we replace the $\{i2\}$ and $\{j2\}$ subscripts with $\{i\}$ and $\{j\}$ subscripts, respectively. For example, under the two-state model, we replace $\tilde{Y}_{i2}$ and $\tilde{Y}_{j2}$ with $\tilde{Y}_i$ and $\tilde{Y}_j$, respectively.

Similarly, using the definitions of the posterior predictive survival distributions under the multistate model, presented in Section C.3 in the supplementary material, we define

$$\rho_i(\tau_i + s|\tau_i, z(\tau_i), \mathcal{D}_n) = \begin{cases} \Pr(T_{i3} \geq \tau_i + s|T_{i3} > \tau_i, z(\tau_i) = 0, \mathcal{D}_n), \\ \text{if drive } i \text{ is in the healthy state at age } \tau_i, \\ \Pr(T_{i3} \geq \tau_i + s|T_{i3} > \tau_i, z(\tau_i) = 1, \mathcal{D}_n), \\ \text{if drive } i \text{ is in the critical 1 state at age } \tau_i, \\ \Pr(T_{i3} \geq \tau_i + s|T_{i3} > \tau_i, z(\tau_i) = 2, \mathcal{D}_n), \\ \text{if drive } i \text{ is in the critical 2 state at age} \tau_i, \end{cases} \tag{36}$$

where $\tau_i$ is the age of drive $i$ at time $\tau$, $z(\tau_i)$ is the state of drive $i$ at age $\tau_i$, $T_{i3}$ is the true failure age of drive $i$, $\mathcal{D}_n$ is the observed data used to obtain the posterior distribution of the multistate model parameters, and the relevant expressions are given in the supplementary material in Equations (C.14)–(C.16), respectively. Under the multistate model, in the definitions of the AUC and the PE, given in Sections 5.1 and 5.2, respectively, we replace the $\{i2\}$ and $\{j2\}$ subscripts with $\{i3\}$ and $\{j3\}$ subscripts, respectively. For example, under the multistate model, we replace $\tilde{Y}_{i2}$ and $\tilde{Y}_{j2}$ with $\tilde{Y}_{i3}$ and $\tilde{Y}_{j3}$, respectively.

## 6 | APPLICATION TO THE BACKBLAZE HARD DRIVES

In this section, we present an analysis of drive model 14. This drive model is chosen to illustrate how multistate models can be used to obtain posterior predictive survival distributions and posterior predictive RUL distributions for hard drives using the age and state of a drive. We show how survival probabilities and RUL distributions are updated, using the age and state of a drive, as additional measurements of the age and critical attributes are recorded. We illustrate how the posterior predictive survival distributions and posterior predictive RUL distributions allow us to define the impact of critical attributes on hard drive survival probabilities and failure ages. In addition, we assess the performance of the two-state model, the illness-death model, and the multistate model using discrimination (AUC) and calibration (PE) measures through a simulation study.

### 6.1 | Drive model 14

Backblaze deployed 4707 model 14 drives. Three of these drives had only one observation and were removed from the dataset. This leaves 4704 hard drives. By the end of 2015, 1707 of these drives had failed. Consequently, 2997 drives are right-censored.

Under the illness-death model, 4341 (92%) hard drives entered the critical state at some point in their lifetime. Although not shown, this model performed poorly. From this model, we observed that as hard drives got older, the probability of failure within a forecast horizon of interest was higher for drives in the healthy state compared to drives in the critical state. This indicated that we misspecified the definition of critical drives. Upon further investigation, we found that 3950 (84%) hard drives experienced at least one nonzero jump in command timeout (SMART 188). A nonzero jump in command timeout did not appear to impact the failure rate of hard drives. Consequently, we removed SMART 188 from the set of critical attributes.

From herein, SMART 5, SMART 187, SMART 197, and SMART 198 are considered critical attributes. Under the illness-death model, with this set of critical attributes, 2428 (52%) hard drives entered the critical state, 283 drives transitioned from the healthy state to the failed state, and 1424 drives transitioned from the critical state to the failed state.

Under the multistate model, 2009 drives transitioned from the healthy state to the critical 1 state, 1316 drives transitioned from the critical 1 state to the critical 2 state, and 419 drives transitioned from the healthy state to the critical 2 state (without transitioning to the critical 1 state). In total 1707 drives failed; 283 drives transitioned from the healthy state to the failed state, 288 hard drives transitioned from the critical 1 state to the failed state, and 1136 drives transitioned from the critical 2 state to the failed state.

We model the failure ages of hard drives using the two-state model (depicted by Figure 1), the illness-death model (depicted by Figure 4), and the multistate model (depicted by Figure 6). We specify the two-state model, the illness-death model, and the multistate model more formally in the next sections.

### 6.2 | Two-state model specifications

In this section we present the two-state model proposed by Mittman et al.[13] Figure 1 depicts the two-state model used to model hard drive failure ages without the inclusion of critical attributes. We assume a two-state model for each individual drive of the form shown in Figure 1. The two-state model is characterized by one transition hazard (see Figure 1 and Equation (1)). A GLFP hazard, described in Section B.2 in the supplementary material, is used to describe the transition rate for hard drives in the healthy state. This model describes the early failure mode and the wear-out failure mode of

hard drives. More specifically,

$$T \sim \text{GLFP}(\pi, t_{p_1}, \sigma_1, t_{p_2}, \sigma_2), \tag{37}$$

where $T$ is the failure age of a hard drive. The transition hazard is obtained using Equations (B.3), (B.4), (B.6), (B.8), and (B.9) in the supplementary material, and is given by

$$\lambda(t|\boldsymbol{\theta}) = \frac{-t^{1/\sigma_1-1}\pi \log(1-p_1)\sigma_1^{-1}t_{p_1}^{-1/\sigma_1} \exp\left[\left(\frac{t}{t_{p_1}}\right)^{1/\sigma_1}\log(1-p_1)\right]}{1-\pi\left(1-\exp\left[\left(\frac{t}{t_{p_1}}\right)^{1/\sigma_1}\log(1-p_1)\right]\right)} - \frac{\log(1-p_2)}{\sigma_2 t_{p_2}}\left(\frac{t}{t_{p_2}}\right)^{1/\sigma_2-1}, \tag{38}$$

where $\boldsymbol{\theta} = (\pi, t_{p_1}, \sigma_1, t_{p_2}, \sigma_2)$. To infer the parameters of the two-state model, we use a Bayesian approach, selecting proper, but generally diffuse, prior distributions to improve the identification of the model parameters. Following Mittman et al.[13] we use the 0.50 quantile for the early failure mode ($p_1 = 0.5$) and the 0.2 quantile for the wear-out failure mode ($p_2 = 0.2$).

The prior distributions used in our analysis are

$$\begin{aligned}
\sigma_1 &\overset{ind.}{\sim} \text{LogNormal}(0,1),\\
\sigma_2 &\overset{ind.}{\sim} \text{LogNormal}(0,1)\ \ \text{Tr}(0,1),\\
t_{p_1} &\overset{ind.}{\sim} \text{LogNormal}(7,1),\\
t_{p_2} &\overset{ind.}{\sim} \text{LogNormal}(10,1),\\
\pi &\overset{ind.}{\sim} \text{LogitNormal}(-3,2),
\end{aligned} \tag{39}$$

where $p_1 = 0.5$ and $p_2 = 0.2$. We truncate the distribution of $\sigma_2$ at 1 (indicated by Tr(0, 1)), restricting the wear-out failure mode to have an increasing hazard function. The two-state model is fit using RStan, the R interface to Stan.[38,39] RStan provides posterior samples from the joint posterior distribution of the model parameters, $p(\boldsymbol{\theta})$, using the prior distributions and the likelihood provided by Equation (2).

## 6.3 | Illness-death model specifications

Figure 4 depicts the illness-death model used to model hard drive failure ages, with the inclusion of critical attributes through the critical state. We assume an illness-death model for each individual drive of the form shown in Figure 4. The illness-death model is characterized by three transition hazards (see Figure 4 and Equations ((6)–(8)).

A GLFP hazard is used to describe the $0 \to 2$ transition and Weibull hazards are used to describe the $0 \to 1$ and $1 \to 2$ transitions, where state 0 is the healthy state, state 1 is the critical state, and state 2 is the failed state (see Figure 4). The hard drives in our dataset enter the critical state after the "early failure" phase and hence hard drives in the critical state are not expected to suffer from the early failure mode. More specifically, the hazard rate for the $0 \to 1$ transition is given by

$$\lambda_{01}(t|\boldsymbol{\theta}_{01}) = -\frac{\log(1-p_{01})}{\sigma_{01}t_{p_{01}}}\left(\frac{t}{t_{p_{01}}}\right)^{1/\sigma_{01}-1}, \tag{40}$$

where $\boldsymbol{\theta}_{01} = (t_{p_{01}}, \sigma_{01})$ and $p_{01} = 0.5$, the hazard rate for the $0 \to 2$ transition is given by

$$\begin{aligned}
\lambda_{02}(t|\boldsymbol{\theta}_{02}) = {} & \frac{-t^{1/\sigma_{1,02}-1}\pi \log(1-p_{1,02})\sigma_{1,02}^{-1}t_{p_{1,02}}^{-1/\sigma_{1,02}} \exp\left[\left(\frac{t}{t_{p_{1,02}}}\right)^{1/\sigma_{1,02}}\log(1-p_{1,02})\right]}{1-\pi\left(1-\exp\left[\left(\frac{t}{t_{p_{1,02}}}\right)^{1/\sigma_{1,02}}\log(1-p_{1,02})\right]\right)}\\
& - \frac{\log(1-p_{2,02})}{\sigma_{2,02}t_{p_{2,02}}}\left(\frac{t}{t_{p_{2,02}}}\right)^{1/\sigma_{2,02}-1},
\end{aligned} \tag{41}$$

where $\boldsymbol{\theta}_{02} = (\pi, t_{p_{1,02}}, \sigma_{1,02}, t_{p_{2,02}}, \sigma_{2,02})$, $p_{1,02} = 0.5$, and $p_{2,02} = 0.2$, and the hazard rate for the $1 \rightarrow 2$ transition is given by

$$\lambda_{12}(t|\boldsymbol{\theta}_{12}) = -\frac{\log(1-p_{12})}{\sigma_{12} t_{p_{12}}} \left(\frac{t}{t_{p_{12}}}\right)^{1/\sigma_{12}-1}, \tag{42}$$

where $\boldsymbol{\theta}_{12} = (t_{p_{12}}, \sigma_{12})$ and $p_{12} = 0.1$.

To infer the parameters of the illness-death model, we use a Bayesian approach, selecting proper, but generally diffuse, prior distributions to improve the identification of the model parameters. The prior distributions for the healthy to failed transition parameters, $\boldsymbol{\theta}_{02}$, are defined in Section 6.2. The remaining prior distributions used in our analysis are

$$\begin{aligned} t_{p_{01}} &\overset{ind.}{\sim} \text{LogNormal}(10, 1), \\ t_{p_{12}} &\overset{ind.}{\sim} \text{LogNormal}(9, 1), \\ \sigma_{01}, \sigma_{12} &\overset{ind.}{\sim} \text{LogNormal}(0, 1)\ \text{Tr}(0, 1). \end{aligned} \tag{43}$$

We truncate the distributions of $\sigma_{01}, \sigma_{2,02}$ and $\sigma_{12}$ at 1, restricting the associated failure modes to have increasing hazard functions. The illness-death model is fit using RStan. RStan provides posterior samples from the joint posterior distribution of the model parameters, $p(\boldsymbol{\theta})$, using the prior distributions and the likelihood provided by Equations (9)–(12).

The likelihood for the illness-death model is given by Equations (9)–(12). The definite integrals in the likelihood in Equations (11) and (12) are evaluated using the composite Simpson's rule with $M = 100$ equal subdivisions. More specifically, for the integral of the general function $f(x|\boldsymbol{\theta})$ over the interval $[0, l_i]$, the evaluation takes the form

$$\int_0^{l_i} f(x|\boldsymbol{\theta})dx = \frac{h}{3}\left\{f(x_0|\boldsymbol{\theta}) + 4\sum_{j=1}^{M/2} f(x_{2j-1}|\boldsymbol{\theta}) + 2\sum_{j=1}^{M/2-1} f(x_{2j}|\boldsymbol{\theta}) + f(x_M|\boldsymbol{\theta})\right\}, \tag{44}$$

where $x_j = jh$, for $j = 0, 1, \ldots, M$, with $h = l_i/M$; in particular, $x_0 = 0$ and $x_M = l_i$.

## 6.4 | Multistate model specifications

Figure 6 depicts the multistate model used to model hard drive failure ages, with the inclusion of critical attributes through the critical 1 and critical 2 states. We assume a multistate model for each individual drive of the form shown in Figure 6. The multistate model is characterized by six transition hazards (see Figure 6 and Equations (17)–(22)). A GLFP hazard is used to describe the $0 \rightarrow 3$ transition, where state 0 is the healthy state and state 3 is the failed state, and Weibull hazards are used to describe all other transitions. More specifically, the hazard rate for the $i \rightarrow j$ transition is given by

$$\lambda_{ij}(t|\boldsymbol{\theta}_{ij}) = -\frac{\log(1-p_{ij})}{\sigma_{ij} t_{p_{ij}}} \left(\frac{t}{t_{p_{ij}}}\right)^{1/\sigma_{ij}-1}, \tag{45}$$

where $\boldsymbol{\theta}_{ij} = (t_{p_{ij}}, \sigma_{ij})$, for $i = 0$ and $j = 1, 2$, for $i = 1$ and $j = 2, 3$, and for $i = 2$ and $j = 3$, and $p_{01} = 0.5$, $p_{02} = 0.05$, $p_{12} = 0.3$, $p_{13} = 0.1$, and $p_{23} = 0.25$. In addition, the hazard rate for the $0 \rightarrow 3$ transition is given by

$$\begin{aligned} \lambda_{03}(t|\boldsymbol{\theta}_{03}) = {} & \frac{-t^{1/\sigma_{1,03}-1}\pi \log(1-p_{1,03})\sigma_{1,03}^{-1} t_{p_{1,03}}^{-1/\sigma_{1,03}} \exp\left[\left(\frac{t}{t_{p_{1,03}}}\right)^{1/\sigma_{1,03}} \log(1-p_{1,03})\right]}{1-\pi\left(1-\exp\left[\left(\frac{t}{t_{p_{1,03}}}\right)^{1/\sigma_{1,03}} \log(1-p_{1,03})\right]\right)} \\ & - \frac{\log(1-p_{2,03})}{\sigma_{2,03} t_{p_{2,03}}} \left(\frac{t}{t_{p_{2,03}}}\right)^{1/\sigma_{2,03}-1}, \end{aligned} \tag{46}$$

where $\boldsymbol{\theta}_{03} = (\pi, t_{p_{1,03}}, \sigma_{1,03}, t_{p_{2,03}}, \sigma_{2,03})$, $p_{1,03} = 0.5$, and $p_{2,03} = 0.2$.

To infer the parameters of the multistate model, we use a Bayesian approach, selecting proper, but generally diffuse, prior distributions to improve the identification of the model parameters. The prior distributions for the healthy to failed transition parameters, $\boldsymbol{\theta}_{03}$, are defined in Section 6.2; and the prior distributions for the healthy to critical 1 transition parameters, $\boldsymbol{\theta}_{01}$, and the critical 1 to failed transition parameters, $\boldsymbol{\theta}_{13}$, are defined in Section 6.3. The remaining prior distributions used in our analysis are

$$\begin{aligned} t_{p_{02}} &\overset{ind.}{\sim} \text{LogNormal}(9,1), \\ t_{p_{12}} &\overset{ind.}{\sim} \text{LogNormal}(9.5,1), \\ t_{p_{23}} &\overset{ind.}{\sim} \text{LogNormal}(9.25,1), \\ \sigma_{02},\sigma_{12},\sigma_{23} &\overset{ind.}{\sim} \text{LogNormal}(0,1)\ \ \text{Tr}(0,1). \end{aligned} \tag{47}$$

We truncate the distributions of $\sigma_{01}, \sigma_{02}, \sigma_{2,03}, \sigma_{12}, \sigma_{13}$ and $\sigma_{23}$ at 1, restricting the associated failure modes to have increasing hazard functions. The multistate model is fit using RStan. RStan provides posterior samples from the joint posterior distribution of the model parameters, $p(\boldsymbol{\theta})$, using the prior distributions and the likelihood provided by Equations (C.7)–(C.13) in the supplementary material.

## 6.5 | Results

### 6.5.1 | Survival probabilities and RUL prediction

Figure 7 illustrates dynamic predictions of conditional survival probabilities over time for hard drives in the healthy state and hard drives in the critical states, obtained under the multistate model using the parameter posterior distributions summarized in Table A.3 in the supplementary material, conditional on surviving until age $\tau_i = 5000, 10000, 15000,$ and 20,000 h. The multistate model allows us to coherently examine the impact of critical attributes on the survival probability of hard drives. The posterior predictive survival distributions can be used to compare the probabilities of failure, within a forecast horizon of interest, of drives in the healthy state to drives in the critical states and to compare the probabilities of failure of drives in the critical 1 state to drives in the critical 2 state. This allows us to concretely define the impact of a single critical attribute, and the impact of multiple critical attributes, on the survival probability of hard drives; which in turn allows us to examine the impact of a single critical attribute and the impact of multiple critical attributes on the RUL distributions of hard drives.

In addition, Figure A.1 illustrates dynamic predictions of conditional survival probabilities over time obtained under the two-state model, using the parameter posterior distributions summarized in Table A.1 in the supplementary material, conditional on surviving until age $\tau_i = 5000, 10{,}000, 15{,}000,$ and 20,000 h. From Figure 7, it appears that the survival probabilities, conditional on surviving until age $\tau_i$, for $\tau_i = 5000, 10{,}000, 15{,}000,$ and 20,000, obtained under the two-state model are a weighted mixture of the three survival curves (corresponding to the survival curves for drives in the healthy, critical 1 and critical 2 states) obtained under the multistate model, conditional on surviving until age $\tau_i$, for $\tau_i = 5000, 10{,}000, 15{,}000, 20{,}000$. In general, the two-state model appears to underestimate the survival probability of drives in the healthy state and overestimate the survival probability of drives in the critical states.

Table 2 provides the posterior median and central posterior 95% prediction intervals of the probability of surviving an 84 day (2016 h) forecast horizon under the two-state model and the multistate model, for drives in the healthy state and drives in the critical states, conditional on surviving until age $\tau_i = 5000, 10{,}000, 15{,}000,$ and 20,000h; 84 days is approximately 3 months (or a quarter of a year) and this is how often Backblaze releases new data. The quantities obtained from the multistate model posterior predictive survival distributions allow us to explicitly identify the impact of a single critical attribute, and the impact of multiple critical attributes, on hard drive survival probabilities. For example, from Table 2, we can see that the median posterior probabilities of surviving an 84 day (2016 h) horizon for a drive of age 20,000 h are 0.9410, 0.7658, and 0.5866 for drives with no critical attributes, one critical attribute and multiple critical attributes, respectively. In addition, under the two-state model, the median posterior probability of surviving an 84 day (2016 h) horizon for a drive of age 20,000 h is 0.8179 regardless of how many critical attributes the drive has acquired.

Figure 8 illustrates the dynamic RUL predictions obtained under the multistate model (for drives in the healthy state, the critical 1 state, and the critical 2 state), using the parameter posterior distributions summarized in Table A.3

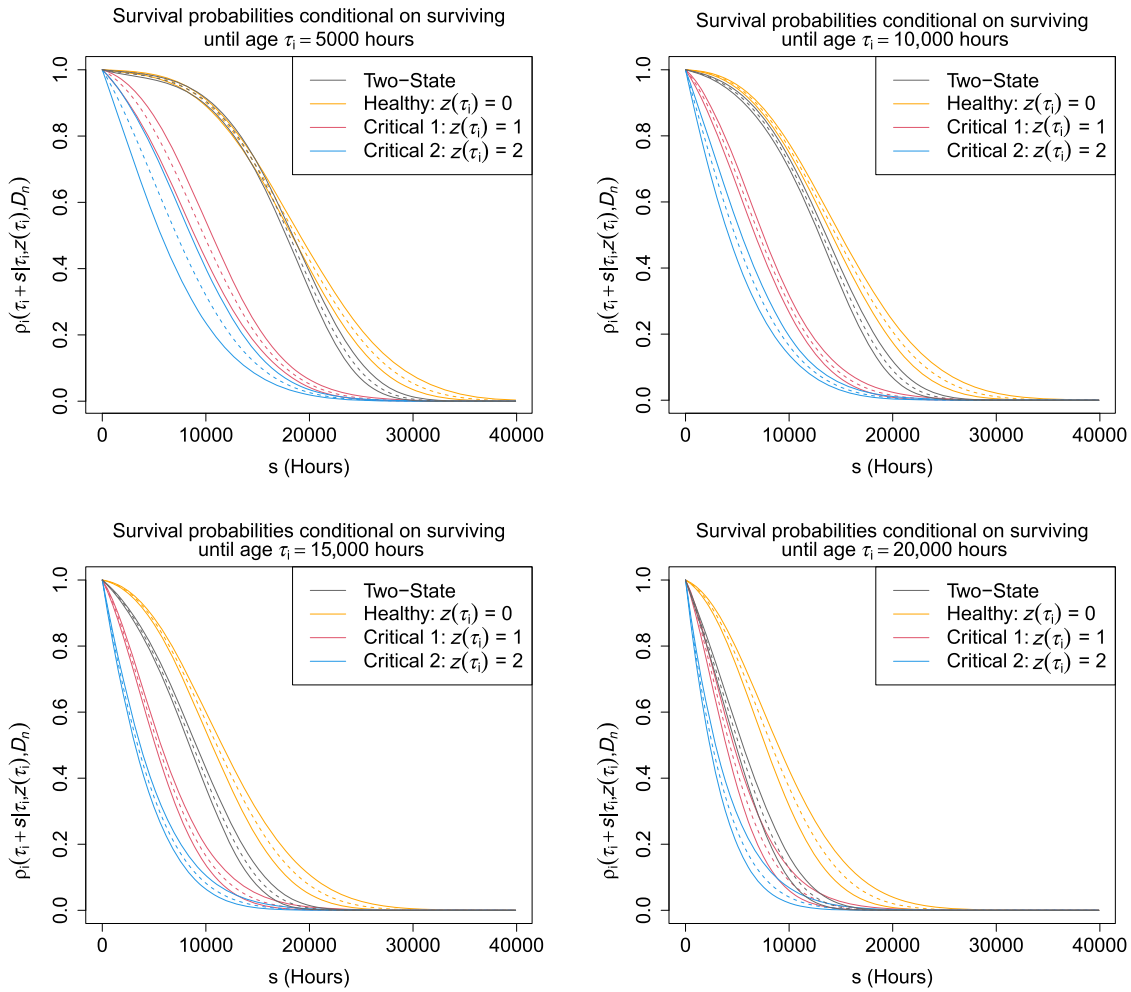


**FIGURE 7** Posterior medians (dashed lines) and 95% central prediction intervals (solid lines) of the survival probability over time under the two-state model (gray) and the multistate model, for hard drives in the healthy state (orange), hard drives in the critical 1 state (red), and hard drives in the critical 2 state (blue), conditional on surviving until age $\tau_i = 5000, 10{,}000, 15{,}000,$ and 20,000 h.

**TABLE 2** Posterior median and central posterior 95% prediction intervals of the probability of surviving an 84 day (2016 h) forecast horizon under the two-state model and the multistate model, for hard drives in the healthy state, drives in the critical 1 state, and drives in the critical 2 state, conditional on surviving until age $\tau_i = 5000, 10{,}000, 15{,}000,$ and 20,000 h.

| Age ($\tau_i$) | Two-State median and 95% PI | Healthy median and 95% PI | Critical 1 median and 95% PI | Critical 2 median and 95% PI |
|---|---|---|---|---|
| 5000 | 0.9910 (0.9866, 0.9941) | 0.9952 (0.9925, 0.9969) | 0.9497 (0.9235, 0.9677) | 0.8793 (0.8160, 0.9223) |
| 10,000 | 0.9815 (0.9787, 0.9839) | 0.9910 (0.9892, 0.9924) | 0.8992 (0.8818, 0.9153) | 0.7748 (0.7298, 0.8130) |
| 15,000 | 0.9308 (0.9256, 0.9355) | 0.9745 (0.9716, 0.9771) | 0.8432 (0.8297, 0.8561) | 0.6768 (0.6536, 0.6993) |
| 20,000 | 0.8179 (0.8050, 0.8309) | 0.9408 (0.9323, 0.9485) | 0.7842 (0.7581, 0.8060) | 0.5874 (0.5543, 0.6230) |

in the supplementary material. Figure 8 provides the RUL predictions, conditional on surviving until age $\tau_i = 5000, 10{,}000, 15{,}000,$ and 20,000 h. As depicted in Figure 8, the RUL, conditional on surviving until age $\tau_i$, for drives in the critical 1 state is lower than the RUL for drives in the healthy state; and the RUL, conditional on surviving until age $\tau_i$, for drives in the critical 2 state is lower than the RUL for drives in the critical 1 state. This illustrates that drives with multiple critical attributes are more prone to failure than drives with only one critical attribute and drives with one critical attribute are more prone to failure than drives without any critical attributes.

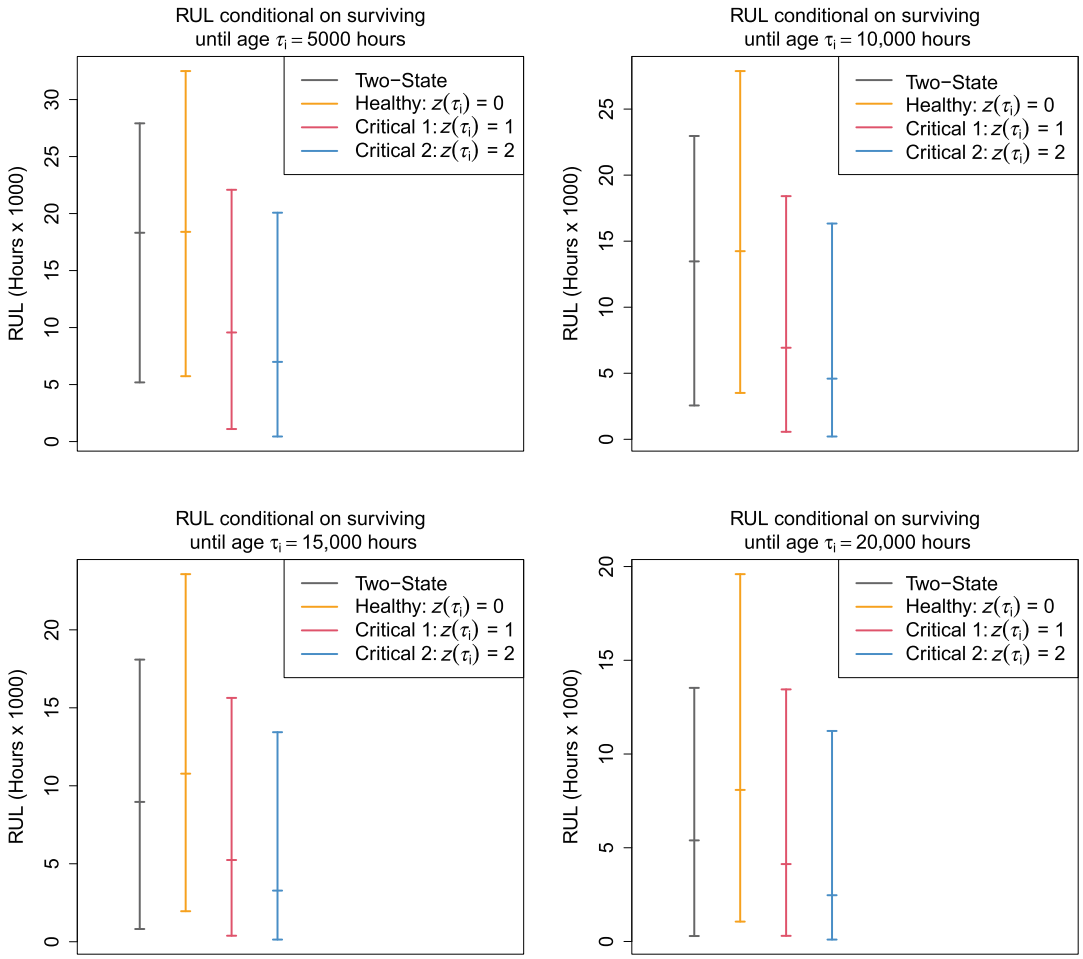


**FIGURE 8** Posterior medians and 95% central prediction intervals of the posterior predictive RUL distributions for hard drives under the two-state model (gray) and the multistate model, for hard drives in the healthy state (orange), hard drives in the critical 1 state (red), and hard drives in the critical 2 state (blue), conditional on surviving until age $\tau_i = 5000, 10{,}000, 15{,}000,$ and 20,000 h. The scales of the y-axes vary between plots.

In addition, Figure 8 illustrates the dynamic RUL predictions obtained under the two-state model, using the parameter posterior distributions summarized in Table A.1 in the supplementary material. From Figure 8, it appears that the RUL distribution, conditional on surviving until age $\tau_i$, for $\tau_i = 5000, 10{,}000, 15{,}000, 20{,}000$, obtained under the two-state model is a weighted mixture of the three RUL distributions (corresponding to the RUL distributions for drives in the healthy, critical 1 and critical 2 states) obtained under the multistate model, conditional on surviving until age $\tau_i$, for $\tau_i = 5000, 10{,}000, 15{,}000, 20{,}000$. The two-state model appears to underestimate the RUL of drives in the healthy state and overestimate the RUL of drives in the critical states. We will assess this more formally in the next section.

The survival probabilities were obtained by sampling from the appropriate posterior predictive survival distributions under each model; and the RUL distributions were obtained by inverse transform sampling from the relevant conditional survival probabilities.

### 6.5.2 | Model assessment

In this section, we investigate the performance of the two-state model, the illness-death model and the multistate model in a simulation study, using the AUC (discrimination) and the PE (calibration) described in Section 5; the square loss function is used to obtain the PE. We obtain the AUC and the PE under all models every 672 h (28 days), assuming three time intervals for prediction of 672 h (28 days), 1344 h (56 days), and 2016 h (84 days), that is, $s = 672, 1344,$ and 2016. More specifically, we obtain the AUC and the PE under all models at the beginning of the study, at calendar time $\tau = 0$, and then at calendar times $\tau = 672, 1344, \ldots$, with $s = 672, 1344,$ and 2016. We perform Monte Carlo cross-validation,

splitting the data into training (60%) and validation (40%) data. For each split, we fit the two-state model, the illness-death model and the multistate model to the training data to obtain the joint posterior distribution of the model parameters under each model. The joint posterior distribution of the model parameters is obtained once under each model using all of the training data. Under each model, we derive dynamic predictions of conditional survival probabilities, using the age and state of a drive, at calendar times $\tau = 672, 1344, \ldots,$ with $s = 672, 1344,$ and 2016. Survival probabilities are dynamically updated, using the age and state of a drive, as additional measurements of the age and critical attributes are recorded. We then obtain the AUC and the PE at each time point and for each forecast horizon, $s$. We run 1000 Monte Carlo simulations.

Tables A.1–A.3 in the supplementary material provide summaries of the parameter posterior distributions for the two-state model, the illness-death model and the multistate model, respectively, for one randomly chosen Monte Carlo cross-validation.

In Figure 9, and Figures A.1 and A.2 in the supplementary material, we present the results of the simulation study, for $s = 672$, 1344, and 2016. Figure 9 presents the results comparing the multistate model to the two-state model; Figure A.1 presents the results comparing the illness-death model to the two-state model; and Figure A.2 presents the results comparing the multistate model to the illness-death model. The calendar times shown were selected based on when the most failures occur in the data.[40]

The boxplots in the top, middle and bottom left panels of Figure 9 represent the difference in the AUC between the multistate model and the two-state model, at multiple time points, for $s = 672, 1344, 2016$, respectively. The boxplots in the top, middle and bottom right panels of Figure 9 represent the difference in the PE between the two-state model and the multistate model. The structure is the same in Figures A.1 and A.2, but these figures compare the illness-death model to the two-state model and the multistate model to the illness-death model, respectively.

From the left panels in Figures 9 and A.1, we can see that the AUC is larger for the multistate model and the illness-death model, compared to the two-state model, at all time points, indicating that the multistate model and the illness-death model are better at discriminating between hard drives than the two-state model. This makes sense since the two-state model does not take into account the effect of obtaining critical attributes. Under the two-state model, the probability of surviving the forecast horizon will always be higher for a "younger" drive. The results shown in the left panels of Figures 9 and A.1 indicate that the multistate model and the illness-death model are able to identify younger drives that are more likely to fail within the relevant time interval, due to these drives being in a critical states.

Moreover, from the right panels in Figures 9 and A.1, we can see that the PE is larger for the two-state model, compared to the multistate model and the illness-death model, at all time points (except for prediction 13 for $s = 672$, where the PE for the two-state model is smaller, compared to the multistate model and the illness-death model; and prediction 9 for $s = 672$ and prediction 13 for $s = 1344$, where the PE for the two-state model is approximately the same as the PE under the illness-death model). This suggests that the multistate model and the illness-death model are more accurate than the two-state model.

Furthermore, from the left panels in Figure A.2, we can see that the AUC is larger for the multistate model, compared to the illness-death model, at all time points (except for prediction 18 for $s = 672, 2016$, where the AUC is slightly larger for the illness-death model compared to the multistate model). This indicates that the multistate model is better at discriminating between hard drives compared to the illness-death model. This makes sense, since the illness-death model does not differentiate between drives with one critical attribute and drives with multiple critical attributes. Under the illness-death model, the probability of surviving the forecast horizon, for a fixed age, is identical for drives with one critical attribute and drives with multiple critical attributes. However, as we can see from Figure 7, drives in the critical 2 state have a lower survival probability at all time points compared to drives in the critical 1 state, meaning drives with multiple critical attributes are more prone to failure than drives with a single critical attribute. The results shown in the left panels of Figure A.2 indicate that the multistate model is able to identify drives that are more likely to fail within the relevant time interval due to these drives having multiple critical attributes rather than a single critical attribute.

Finally, from the right panels in Figure A.2, we can see that the PE is larger for the illness-death model, compared to the multistate model, at all time points. This suggests that the multistate model is more accurate than the illness-death model.

We note that the differences in the AUC and the PE between the multistate model and the illness-death model are not as large as the differences between the multistate model and the two-state model or between the illness-death model and the two-state model (see the scales in Figures 9 and A.1 compared to Figure A.2). This suggests that more complex models, for example, a multistate model with five states (with three critical states), may not be superior to the four-state

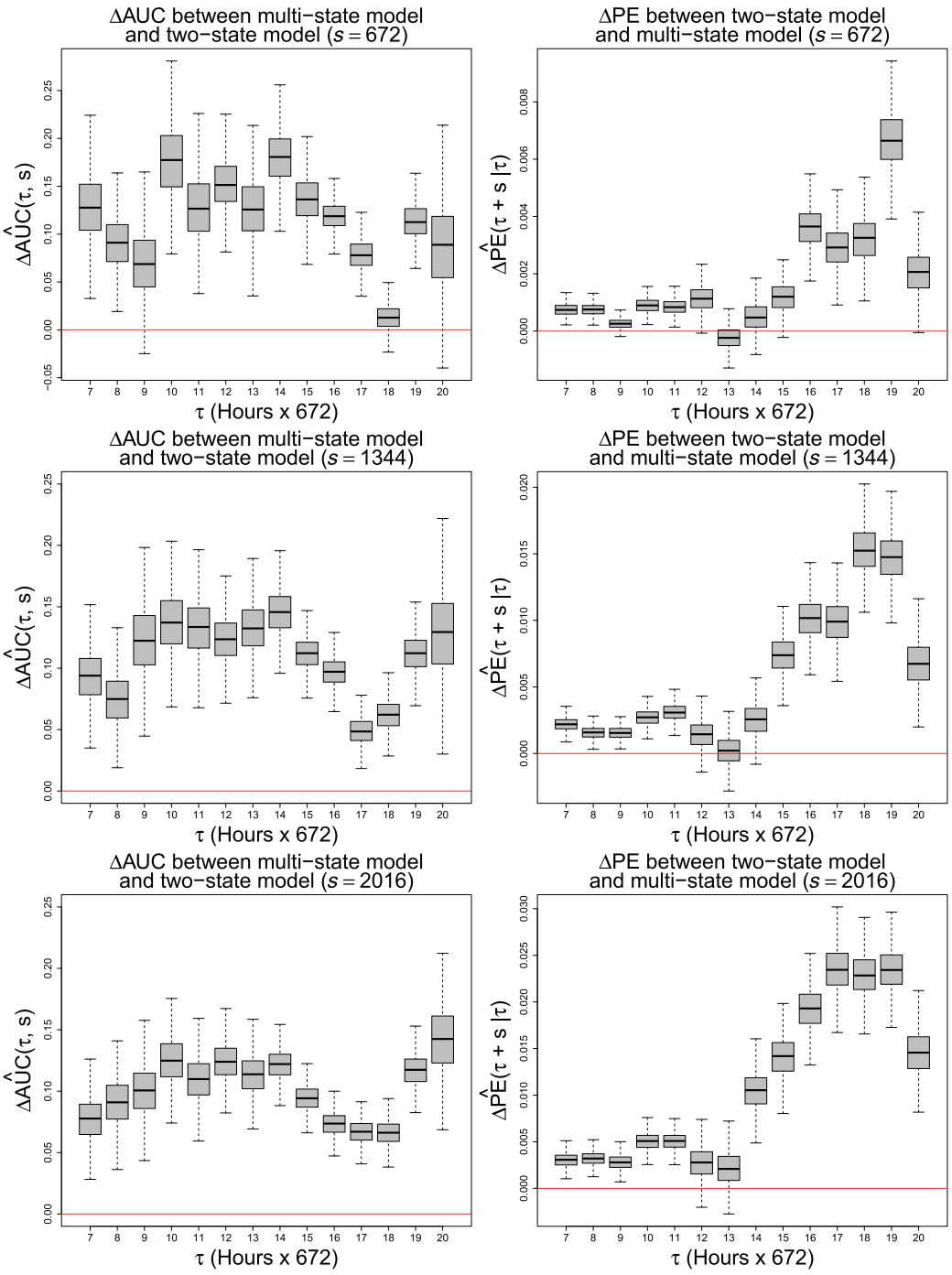


**FIGURE 9** Top, middle and bottom left panels show the difference in the AUC, at multiple time points, between the multistate model and the two-state model, for $s =$ 672, 1344, and 2016, respectively. Top, middle and bottom right panels show the difference in the PE, at multiple time points, between the two-state model and the multistate model, for $s = 672$, 1344, and 2016, respectively. The scales of the $y$-axes vary between plots.

multistate model presented in this article. In addition, this model would have more parameters and be more challenging to train (due to fewer drives transitioning between each state).

## 7 | CONCLUSION

In this article, we proposed a coherent and novel way to use data collected by SMART to obtain posterior predictive survival distributions and posterior predictive RUL distributions for hard drives; and we examined the impact of a single

critical attribute and the impact of multiple critical attributes on hard drive failure ages. We illustrated how to obtain dynamic predictions and showed how survival probabilities are updated, using the age and state of a drive, as additional measurements of the age and critical attributes are recorded.

Following from Ma et al.,[6] Rincón et al.,[30] and Backblaze[31] we reduced the number of SMART attributes to a reduced set of "critical" attributes. A parametric model for the critical attributes is needed for the purpose of prediction. However, the evolution of each critical attribute is poorly understood, and it is challenging to predict the values of the critical attributes over time. To overcome this problem, we proposed critical states for hard drives using the critical attributes. Under our definition of the critical states, we do not need to forecast the process for any critical attribute. Instead, we must forecast the probability of entering the critical states. It is challenging to predict the value of critical attributes over time, but it is more manageable to obtain the probability of entering the critical states. This provided a framework for incorporating the erratic critical attributes.

We modeled the semi-competing risks data using the illness-death model and the multistate model, and examined the impact of critical attributes on hard drive survival probabilities and failure ages. The proposed models provided a coherent and novel way to model the failure ages of hard drives while incorporating the attributes provided by SMART.

We illustrated the multistate modeling approach using a dataset of hard drives that is left-truncated and right-censored. We proposed transition-specific hazard functions for each event. We used the GLFP model to model the probability of failure for drives in the healthy state. The GLFP model described the early failure mode due to manufacturing defects and captured the wear-out failures observed after the initial "burn-in" period. Weibull hazards were used to describe the transitions between all other states.

We investigated the impact of critical attributes on hard drive failure ages using the multistate model. We found that the RUL for drives was impacted by a single critical attribute and impacted further by multiple critical attributes. The RUL, conditional on surviving until age $\tau_i = 5000, 10{,}000, 15{,}000,$ and $20{,}000$ h, for drives in the critical 1 state was lower than the RUL for drives in the healthy state; and the RUL, conditional on surviving until age $\tau_i = 5000, 10,000, 15,000,$ and $20,000$ h, for drives in the critical 2 state was lower than the RUL for drives in the critical 1 state. This illustrated that drives with multiple critical attributes are more prone to failure than drives with only one critical attribute and drives with one critical attribute are more prone to failure than drives without any critical attributes. We obtained the posterior predictive survival probabilities over time, conditional on surviving until age $\tau_i = 5000, 10,000, 15,000,$ and $20,000$ h, for drives with no critical attributes (drives in the healthy state), for drives with one critical attribute (drives in the critical 1 state) and for drives with multiple critical attributes (drives in the critical 2 state). The posterior predictive survival curves allow us to concretely define the impact of a single critical attribute and the impact of multiple critical attributes on the survival probabilities of a hard drive, which in turn allows us to examine the impact of a single critical attribute and the impact of multiple critical attributes on the RUL of a hard drive.

We assessed the performance of the multistate model using discrimination (AUC) and calibration (PE) measures, comparing predictions obtained from the multistate model to the illness-death model and the two-state model. We performed Monte Carlo cross-validation, splitting the data into training (60%) and validation (40%) data. For each split, we fitted the two-state model, the illness-death model and the multistate model to the training data. We obtained the AUC and the PE every four weeks (672 h), assuming relevant time intervals of $s = 672, 1344,$ and $2016$ h for prediction. We found that the multistate model and the illness-death model outperformed the two-state model. Furthermore, we found that the multistate model outperformed the illness-death model. The results illustrated the importance of incorporating data collected by SMART, and the multistate model provided a framework to do this.

The differences in the AUC and the PE between the multistate model and the illness-death model were not as large as the differences between the multistate model and the two-state model or between the illness-death model and the two-state model. This suggested that more complex models, for example, a multistate model with five states, may not be superior to the four-state multistate model presented in this article.

Furthermore, unlike Rincón et al.,[30] and Backblaze,[31] we found that command timeout, SMART 188, did not appear to impact the failure rate of a hard drive.

## ACKNOWLEDGMENTS

This work was supported by the Engineering and Physical Sciences Research Council, Centre for Doctoral Training in Cloud Computing for Big Data (grant number EP/L015358/1).

## DATA AVAILABILITY STATEMENT

The data that support the findings of this study are openly available at https://www.backblaze.com/b2/hard-drive-test-data.html.

## REFERENCES


1. Hong Y, Meeker WQ. Field-failure predictions based on failure-time data with dynamic covariate information. *Technometrics*. 2013;55(2):135-149.
2. Manousakis I, Sankar S, McKnight G, Nguyen TD, Bianchini R. Environmental conditions and disk reliability in free-cooled datacenters. *14th USENIX Conference on File and Storage Technologies (FAST'16)*. USENIX Association; 2016:53-65.
3. Vishwanath KV, Nagappan N. Characterizing cloud computing hardware reliability. *Proceedings of the 1st ACM Symposium on Cloud Computing*. Association for Computing Machinery; 2010:193-204.
4. Murray JF, Hughes GF, Kreutz-Delgado K, Schuurmans D. Machine learning methods for predicting failures in hard drives: a multiple-instance application. *J Mach Learn Res*. 2005;6(5):783-816.
5. Lu S, Luo B, Patel T, Yao Y, Tiwari D, Shi W. Making disk failure predictions SMARTer! *18th USENIX Conference on File and Storage Technologies (FAST'20)*. USENIX Association; 2020:151-167.
6. Ma A, Traylor R, Douglis F, et al. Raidshield: characterizing, monitoring, and proactively protecting against disk failures. *ACM Trans Storage*. 2015;11(4):1-28.
7. Pinheiro E, Weber W-D, Barroso LA. Failure trends in a large disk drive population. *5th USENIX Conference on File and Storage Technologies (FAST'07)*. USENIX Association; 2007:17-29.
8. Chhetri TR, Kurteva A, Adigun JG, Fensel A. Knowledge graph based hard drive failure prediction. *Sensors*. 2022;22(3):985.
9. Cahyadi M. Forshaw, Hard disk failure prediction on highly imbalanced data using LSTM network. *2021 IEEE International Conference on Big Data (Big Data)*. IEEE; 2021:3985-3991. doi:10.1109/BigData52589.2021.9671555
10. Backblaze hard drive data sets. https://www.backblaze.com/b2/hard-drive-test-data.html
11. Botezatu MM, Giurgiu I, Bogojeska J, Wiesmann D. Predicting disk replacement towards reliable data centers. *Proceedings of the 22nd ACM SIGKDD International Conference on Knowledge Discovery and Data Mining*. Association for Computing Machinery; 2016:39-48.
12. Shen J, Wan J, Lim S-J, Yu L. Random-forest-based failure prediction for hard disk drives. *Int J Distrib Sensor Netw*. 2018;14(11):1-15.
13. Mittman E, Lewis-Beck C, Meeker WQ. A hierarchical model for heterogenous reliability field data. *Technometrics*. 2019;61(3):354-368.
14. Chaves IC, De Paula MRP, Leite LG, Gomes JPP, Machado JC. Hard disk drive failure prediction method based on a bayesian network. *2018 International Joint Conference on Neural Networks (IJCNN)*. IEEE; 2018:1-7.
15. dos Santos Lima FD, Amaral GMR, de Moura Leite LG, Gomes JPP, de Castro Machado J. Predicting failures in hard drives with lstm networks. *2017 Brazilian Conference on Intelligent Systems (BRACIS)*. IEEE; 2017:222-227.
16. Fine JP, Jiang H, Chappell R. On semi-competing risks data. *Biometrika*. 2001;88(4):907-919.
17. Xu J, Kalbfleisch JD, Tai B. Statistical analysis of illness–death processes and semicompeting risks data. *Biometrics*. 2010;66(3):716-725.
18. Varadhan R, Xue Q-L, Bandeen-Roche K. Semicompeting risks in aging research: methods, issues and needs. *Lifetime Data Anal*. 2014;20(4):538-562.
19. Peng L, Fine JP. Regression modeling of semicompeting risks data. *Biometrics*. 2007;63(1):96-108.
20. Hsieh J-J, Wang W, Adam Ding A. Regression analysis based on semicompeting risks data. *J R Statist Soc: Ser B*. 2008;70(1):3-20.
21. Lakhal L, Rivest L-P, Abdous B. Estimating survival and association in a semicompeting risks model. *Biometrics*. 2008;64(1):180-188.
22. Egleston BL, Scharfstein DO, Freeman EE, West SK. Causal inference for non-mortality outcomes in the presence of death. *Biostatistics*. 2007;8(3):526-545.
23. Tchetgen Tchetgen EJ. Identification and estimation of survivor average causal effects. *Stat Med*. 2014;33(21):3601-3628.
24. Liu L, Wolfe RA, Huang X. Shared frailty models for recurrent events and a terminal event. *Biometrics*. 2004;60(3):747-756.
25. Putter H, Fiocco M, Geskus RB. Tutorial in biostatistics: competing risks and multi-state models. *Stat Med*. 2007;26(11):2389-2430.
26. Lee KH, Haneuse S, Schrag D, Dominici F. Bayesian semiparametric analysis of semicompeting risks data: investigating hospital readmission after a pancreatic cancer diagnosis. *J R Stat Soc: Ser C*. 2015;64(2):253-273.
27. Lee C, Lee SJ, Haneuse S. Time-to-event analysis when the event is defined on a finite time interval. *Stat Methods Med Res*. 2020;29(6):1573-1591.
28. Lee C, Gilsanz P, Haneuse S. Fitting a shared frailty illness-death model to left-truncated semi-competing risks data to examine the impact of education level on incident dementia. *BMC Med Res Methodol*. 2021;21(1):1-13.
29. Vakulenko-Lagun B, Mandel M. Comparing estimation approaches for the illness–death model under left truncation and right censoring. *Stat Med*. 2016;35(9):1533-1548.
30. Rincón CA, Pâris J-F, Vilalta R, Cheng AM, Long DD. Disk failure prediction in heterogeneous environments. *2017 International Symposium on Performance Evaluation of Computer and Telecommunication Systems (SPECTS)*. Vol 2017. IEEE; 2017:1-7.
31. Backblaze. What smart stats tell us about hard drives. 2022. https://www.backblaze.com/blog/what-smart-stats-indicat%25%20e-hard-drive-failures
32. Schemper M, Henderson R. Predictive accuracy and explained variation in cox regression. *Biometrics*. 2000;56(1):249-255.
33. Gerds TA, Schumacher M. Consistent estimation of the expected brier score in general survival models with right-censored event times. *Biometr J*. 2006;48(6):1029-1040.

34. Harrell FE Jr, Lee KL, Mark DB. Multivariable prognostic models: issues in developing models, evaluating assumptions and adequacy, and measuring and reducing errors. *Stat Med*. 1996;15(4):361-387.
35. Proust-Lima C, Taylor JM. Development and validation of a dynamic prognostic tool for prostate cancer recurrence using repeated measures of posttreatment psa: a joint modeling approach. *Biostatistics*. 2009;10(3):535-549.
36. Rizopoulos D, Molenberghs G, Lesaffre EM. Dynamic predictions with time-dependent covariates in survival analysis using joint modeling and landmarking. *Biometr J*. 2017;59(6):1261-1276.
37. Henderson R, Diggle P, Dobson A. Identification and efficacy of longitudinal markers for survival. *Biostatistics*. 2002;3(1):33-50.
38. Carpenter B, Gelman A, Hoffman MD, et al. Stan: a probabilistic programming language. *J Stat Softw*. 2017;76(1):1-32.
39. Stan. Stan documentation. 2022 https://mc-stan.org/users/documentation
40. Papageorgiou G, Mokhles MM, Takkenberg JJ, Rizopoulos D. Individualized dynamic prediction of survival with the presence of intermediate events. *Stat Med*. 2019;38(30):5623-5640.

## SUPPORTING INFORMATION

Additional supporting information can be found online in the Supporting Information section at the end of this article.

**How to cite this article:** Oakley JL, Forshaw M, Philipson P, Wilson KJ. Examining the impact of critical attributes on hard drive failure times: Multi-state models for left-truncated and right-censored semi-competing risks data. *Appl Stochastic Models Bus Ind*. 2023;1-26. doi: 10.1002/asmb.2829